Natural Resources Canada
Ressources naturelles Canada

Insight on the chemostratigraphy of the volcanic and intrusive rocks of the Lalor auriferous volcanogenic massive-sulphide deposit host succession, Snow Lake, Manitoba

A. Caté, P. Mercier-Langevin, P.-S. Ross, S. Duff, M. Hannington, S. Gagné, and B. Dubé

Geological Survey of Canada
Current Research 2014-6

2014

Canada

Geological Survey of Canada
Current Research 2014-6

Insight on the chemostratigraphy of the volcanic and intrusive rocks of the Lalor auriferous volcanogenic massive-sulphide deposit host succession, Snow Lake, Manitoba

A. Caté, P. Mercier-Langevin, P.-S. Ross, S. Duff, M. Hannington, S. Gagné, and B. Dubé

2014

ISSN 1701-4387
Catalogue No. M44-2014/6E-PDF
ISBN 978-1-100-24859-2
doi: 10.4095/295080

A copy of this publication is also available for reference in depository libraries across Canada through access to the Depository Services Program's Web site at http://dsp-psd.pwgsc.gc.ca

This publication is available for free download through GEOSCAN http://geoscan.ess.nrcan.gc.ca

Recommended citation

Caté, A., Mercier-Langevin, P., Ross, P.-S., Duff, S., Hannington, M, Gagné, S., and Dubé, B., 2014. Insight on the chemostratigraphy of the volcanic and intrusive rocks of the Lalor auriferous volcanogenic massive-sulphide deposit host succession, Snow Lake, Manitoba; Geological Survey of Canada, Current Research 2014-6, 19 p. doi: 10.4095/295080

Critical review
J. Peter

Authors

A. Caté (antoine.cate@ete.inrs.ca)
P.-S. Ross (Pierre-Simon.Ross@ete.inrs.ca)
Institut national de la recherche scientifique–Centre Eau, Terre et Environnement
490, rue de la Couronne
Québec, Quebec G1K 9A9

P. Mercier-Langevin (Patrick.Mercier-Langevin@RNCan-NRCan.gc.ca)
B. Dubé (Benoit.Dube@RNCan-NRCan.gc.ca)
Geological Survey of Canada
490, rue de la Couronne
Québec, Quebec G1K 9A9

S. Duff (sduff088@uottawa.ca)
M. Hannington (Mark.Hannington@uottawa.ca)
Department of Earth Sciences
University of Ottawa
140 Louis-Pasteur
Ottawa, Ontario K1N 6N5

S. Gagné (Simon.Gagne@gov.mb.ca)
Manitoba Geological Survey
Unit 360, 1395 Ellice Avenue
Winnipeg, Manitoba R3G 3P2

Correction date:

Insight on the chemostratigraphy of the volcanic and intrusive rocks of the Lalor auriferous volcanogenic massive-sulphide deposit host succession, Snow Lake, Manitoba

A. Caté, P. Mercier-Langevin, P.-S. Ross, S. Duff,
M. Hannington, S. Gagné, and B. Dubé

Caté, A., Mercier-Langevin, P., Ross, P.-S., Duff, S., Hannington, M, Gagné, S., and Dubé, B., 2014. Insight on the chemostratigraphy of the volcanic and intrusive rocks of the Lalor auriferous volcanogenic massive-sulphide deposit host succession, Snow Lake, Manitoba; Geological Survey of Canada, Current Research 2014-6, 19 p. doi:10.4095/295080

Abstract: Lalor is a recently discovered auriferous Zn-Cu volcanogenic massive-sulphide deposit. It is located in the Paleoproterozoic Snow Lake arc assemblage, host to numerous past producing Cu-Zn and Zn-Cu volcanogenic massive-sulphide deposits. With an estimated tonnage of 25 Mt of ore (reserves+resources) including 73 t Au, Lalor is the largest volcanogenic massive-sulphide deposit in the Snow Lake area and its Au-rich nature provides a unique opportunity to document processes responsible for precious-metal enrichment in volcanogenic massive-sulphide systems. The Lalor deposit host rocks are predominantly volcanic (± intrusive) rocks that have been variably altered, deformed, and metamorphosed to amphibolite grade. A combination of immobile element geochemistry and petrographic observations is necessary to properly characterize the volcanic rocks due to major postemplacement modifications. Seven distinct chemostratigraphic units and two postvolcanogenic massive-sulphide intrusive (dyke) units are present in the Lalor host succession. Mafic to felsic volcanic units have calc-alkaline to transitional magmatic affinities. Some of these units are compositionally similar to the Moore basalt (units M1a and M1b) and Powderhouse dacite (unit F2) which represent the footwall of the Chisel, Chisel North, Ghost, and Lost volcanogenic massive-sulphide deposits; this suggests that the Lalor deposit is located within the volcanogenic massive-sulphide–fertile uppermost portion of the lower Chisel subsequence. The presence of massive-sulphide ore lenses in calc-alkaline mafic rocks lying above the Powderhouse dacite–like unit indicates the continuation of volcanogenic massive-sulphide–forming hydrothermal activity after the cessation of felsic volcanism in the lower Chisel subsequence. The presence of dykes with a trace-element signature similar to that of the Threehouse basalt, which is present immediately above the other volcanogenic massive-sulphide deposits of the lower Chisel subsequence, suggests the presence of this unit at a higher stratigraphic position in the now structurally truncated sequence.

Résumé : Le gisement de Lalor, récemment découvert, est un gisement de sulfures massifs volcanogènes aurifères à Zn-Cu. Il est situé dans l'assemblage d'arc de Snow Lake du Paléoprotérozoïque, qui renferme de nombreux gisements de sulfures massifs volcanogènes à Cu-Zn et Zn-Cu autrefois exploités. Avec un tonnage estimé à 25 Mt de minerai (réserves + ressources), y compris 73 t de Au, Lalor est le plus important gisement de sulfures massifs volcanogènes dans la région de Snow Lake, et sa richesse en or offre une occasion unique de documenter les processus d'enrichissement en métaux précieux dans les systèmes de sulfures massifs volcanogènes. Les roches encaissantes du gisement de Lalor sont surtout des roches volcaniques (±intrusives) qui, de façon variable, ont été altérées, déformées et métamorphisées au faciès des amphibolites. Une combinaison de la géochimie des éléments immobiles et d'observations pétrographiques est nécessaire afin de caractériser convenablement les roches volcaniques en raison de modifications majeures survenues après leur mise en place. Sept unités chimiostratigraphiques distinctes et deux unités intrusives (dykes) postérieures à la minéralisation de sulfures massifs volcanogènes sont présentes dans la succession encaissante du gisement de Lalor. Les unités volcaniques mafiques à felsiques présentent des affinités magmatiques calco-alcalines à transitionnelles. Certaines de ces unités ont une composition semblable à celle du basalte de Moore (unités M1a et M1b) et de la dacite de Powderhouse (unité F2) qui représentent l'éponte inférieure des gisements de sulfures massifs de Chisel, de Chisel North, de Ghost et de Lost, ce qui donne à penser que le gisement de Lalor est situé dans la partie sommitale fertile en sulfures massifs volcanogènes de la sous-séquence inférieure de Chisel. La présence de lentilles minéralisées de sulfures massifs dans des roches mafiques calco-alcalines qui surmontent l'unité s'apparentant à la dacite de Powderhouse indique la continuation de l'activité hydrothermale responsable de la formation de sulfures massifs volcanogènes après la fin du volcanisme felsique dans la sous-séquence inférieure de Chisel. La présence de dykes affichant une signature en éléments en traces semblable à celle du basalte de Threehouse, qui se trouve directement au-dessus des autres gisements de sulfures massifs volcanogènes de la sous-séquence inférieure de Chisel, laisse croire que cette unité se situe à une position stratigraphique plus élevée dans la séquence qui est maintenant structuralement tronquée.

INTRODUCTION

An understanding of the volcanic successions that host volcanogenic massive-sulphide deposits is critical in understanding their genesis and developing exploration models (e.g. Gibson et al., 1999). The physical and compositional nature of host rocks influences the style and composition of volcanogenic massive-sulphide deposits, which tend to occur along certain key stratigraphic horizons. Therefore, understanding the volcanic stratigraphy is critical for effective exploration at camp scale; however, volcanogenic massive-sulphide–associated hydrothermal alteration, and subsequent metamorphism and deformation commonly obliterate primary textural and mineralogical characteristics of the volcanic rocks (e.g. Bernier et al., 1987; Gifkins et al., 2005; Mercier-Langevin et al., 2007a; Zheng et al., 2011). Whole-rock lithogeochemistry, and more particularly, relatively immobile element geochemistry are critical to deciphering the primary volcanic stratigraphy of volcanogenic massive-sulphide–bearing successions (e.g. Galley et al., 1993; MacLean and Barrett, 1993; Barrett and MacLean, 1999; Mercier-Langevin et al., 2007a, b; Zheng et al., 2011).

The Lalor deposit, located in the Snow Lake district in northern Manitoba, is hosted in volcanic and subvolcanic rocks that have undergone a complex and intense hydrothermal alteration history (Caté et al., 2013b), amphibolite-grade metamorphism (Froese and Gasparrini, 1975; Lam et al., 2013, 2014; Tinkham, 2013), and major deformation events (David et al., 1996; Kraus and Williams, 1999); however, in order to simplify the reading, volcanic names of rocks will be used in this report, instead of metamorphic names (e.g. rhyolite instead of metarhyolite). The Lalor deposit has combined reserves and resources of 25.3 Mt at 0.79% Cu, 5% Zn, 2.90 g/t Au, and 27.1 g/t Ag (as of January 2014; Hudbay Minerals Inc., 2014). This includes 8.8 Mt at 4.6 g/t Au. Due to its large size and major gold endowment (~80.1 t Au (2.6 Moz Au)), the Lalor deposit represents an important opportunity to study the processes responsible for precious-metal enrichment in this deposit, and, by inference, other volcanogenic massive-sulphide deposits.

This research at Lalor is part of a doctoral study conducted at the Institut national de la recherche scientifique, Centre Eau, Terre et Environnement, co-funded by the Geological Survey of Canada Targeted Geoscience Initiative 4, and Hudbay Minerals Inc. The objective of the Lalor study is to characterize the volcanic stratigraphy, hydrothermal alteration, ore-forming processes, and tectonic history of the deposit. This will contribute to the genetic and exploration model for Au-rich volcanogenic massive-sulphide deposits in Canada and elsewhere.

Herein the authors present the volcanic stratigraphy of the Lalor host succession, as determined by drill-core logging and sampling, whole-rock lithogeochemistry, and underground mapping. Other aspects of the Lalor deposit geology and genesis will be presented in separate contributions.

REGIONAL GEOLOGICAL SETTING

The Lalor and Snow Lake camp volcanogenic massive-sulphide deposits are located in the eastern part of the Paleoproterozoic Flin Flon greenstone belt, Manitoba (Fig. 1). The Flin Flon belt is known for its base-metal and gold endowment within numerous volcanogenic massive-sulphide (e.g. the giant Flin Flon deposit, Koo and Mossman (1975)) and orogenic gold deposits and prospects (Galley et al., 2007). The Flin Flon belt is part of the juvenile portion of the Trans-Hudson Orogen (Corrigan et al., 2009), and is divided in three distinct areas: the western Hanson Lake block, the central Amisk collage, and the eastern Snow Lake allochton (Fig. 1; Galley et al., 2007). The belt consists of 1.92–1.87 Ga pre-accretion-arc and ocean-floor assemblages, 1.89–1.83 Ga successor arc and related plutons, 1.88–1.83 Ga sedimentary rocks, and 1.82–1.76 Ga postcollision granite (David et al., 1996; Lucas et al., 1996; Zwanzig, 1999).

The Snow Lake arc assemblage (Snow Lake allochton) can be subdivided into three volcanic sequences that were formed at discrete evolutionary stages of arc development from: a primitive arc (Anderson sequence); a mature arc (Chisel sequence); and arc rifting (Snow Creek sequence) (Fig. 2; Bailes and Galley, 1999).

The Anderson primitive arc sequence hosts Cu-rich, bimodal mafic–type volcanogenic massive-sulphide deposits, including the Anderson Lake and Stall Lake deposits, which are associated with rhyolite complexes (Bailes and Galley, 1999; Galley et al., 2007).

The Chisel mature arc sequence hosts Zn-rich, bimodal felsic–type volcanogenic massive-sulphide deposits located at the contact between the lower and upper part of the sequence (Bailes and Galley, 1999; Galley et al., 2007). The Chisel, Chisel North, Ghost, and Lost deposits are spatially and temporally associated with rhyolite domes and are located at the contact between the footwall Powderhouse dacite and the hanging-wall Threehouse basalt and volcaniclastic rocks (Fig. 2; Galley et al., 2007). The contact between the footwall and hanging wall at Chisel, Chisel North, Ghost, and Lost deposits demarcates the transition between the lower Chisel and upper Chisel subsequences; however, this contact may in part be structural (i.e. Chisel-Lalor thrust, A.H. Bailes (Hudbay Minerals Inc. unpub. internal report, 2011)) as well as stratigraphic (Engelbert et al., 2014). The Lalor deposit is also thought to be situated along this contact (Bailes et al., 2013) based on geochemical similarities between the Lalor footwall rocks and the footwall rocks at Chisel and Chisel North deposits (A.H. Bailes, Hudbay Minerals Inc. unpub. internal report, 2009); however, detailed works suggest some differences between the footwall successions at Lalor and the other volcanogenic massive-sulphide deposits of the lower Chisel subsequence (Bailes et al., 2013; Caté et al., 2013b).

The Chisel sequence is overlain by the Snow Creek sequence that marks the end of arc volcanism and the beginning of arc rifting (Bailes and Galley, 1999). The Snow Creek sequence contains no volcanogenic massive-sulphide deposits or occurrences.

The Snow Lake arc assemblage is affected by at least four episodes of deformation related to the Trans-Hudson Orogeny that are responsible for fold-and-thrust–style stacking and interleaving of the volcanic sequences with younger sedimentary rocks of the Kisseynew Domain (Kraus and Williams, 1999). The recognized D_1 and D_2 events formed tight, isoclinal, southerly verging folds and shallowly dipping thrusts responsible for the development of the main foliation (Kraus and Williams, 1999; Bailes et al., 2013). These structures are refolded by F_3 folds with north-northeast–south-southwest axes with the local presence of an S_3 crenulation cleavage (Kraus and Williams, 1999). F_4 folds are locally observed with east-west axes that affect F_3 folds (Kraus and Williams, 1999).

In the Lalor deposit area, D_{1-2} and D_3 features are strongly developed. North-south–oriented shear zones crosscutting the mineralization underground have also been mapped, but their association with regional deformation events is still unclear. Ongoing work, including the present study, aims at unravelling the complex structural history of the deposit and the effects of deformation on the geometry of the ore zones and distribution of metals.

GEOLOGY OF THE LALOR DEPOSIT

The Lalor deposit is hosted within a strongly altered volcanic succession (Lalor volcanic succession), which was metamorphosed to amphibolite grade (Fig. 3). The host succession units are generally oriented parallel to the main foliation and dip to the northeast. Another discrete volcanic succession is located above the Lalor succession herein referred to as the Balloch volcanic succession (Fig. 3). The contact between the two successions succession is structural and dips shallowly (<10°) toward the north-northeast, whereas units situated above the structural contact dip steeply toward the northeast (A.H. Bailes,

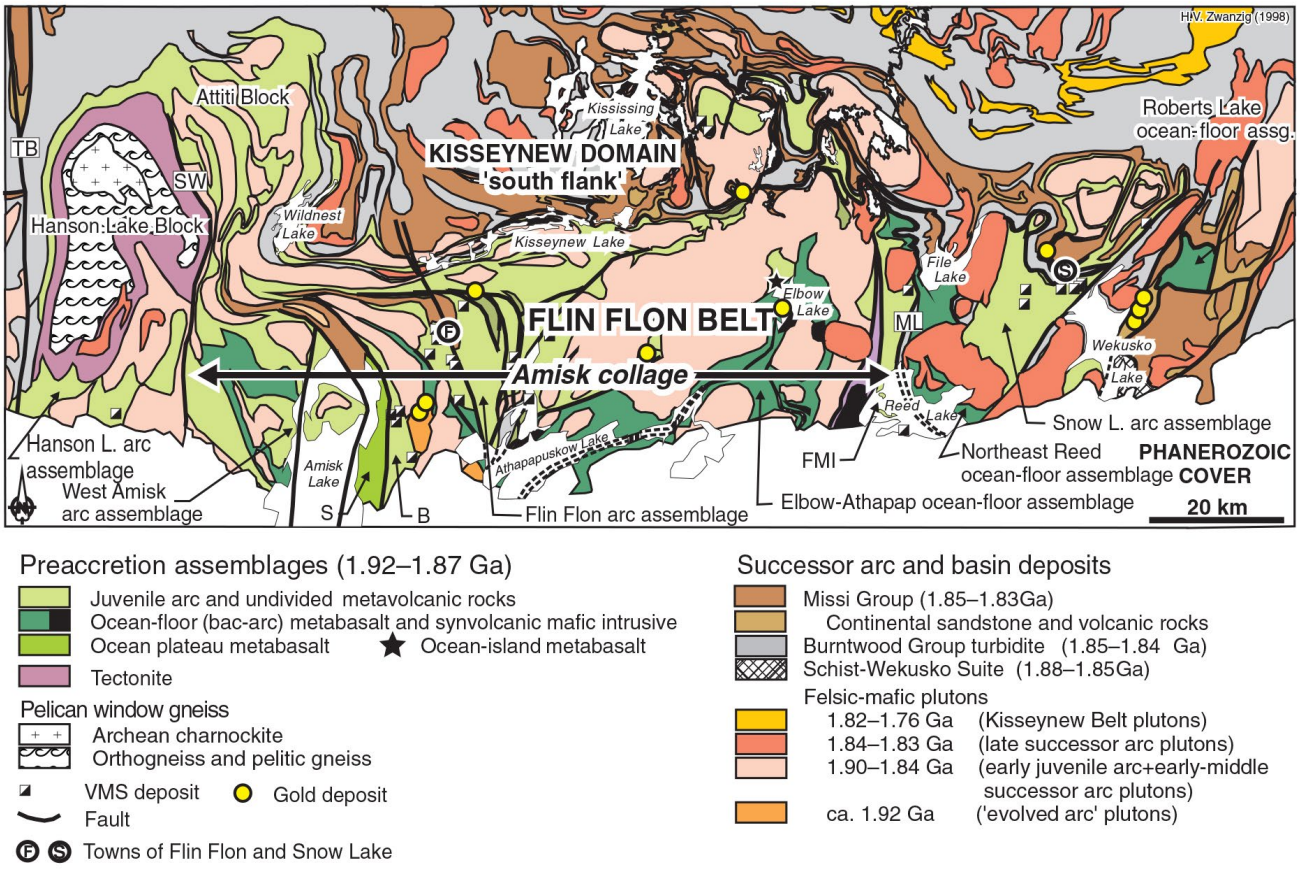

Figure 1. Map of the Flin Flon belt, illustrating the tectonic-stratigraphic assemblages, the location of the various accretionary assemblages, and the major mineral deposits. B = Birch Lake assemblage, FMI = Fourmile Island assemblage, ML = Morton Lake fault zone, S = Sandy Bay assemblage, TB = Tabernor fault zone, SW = Sturgeon-Weir fault zone, VMS = volcanogenic massive sulphide, assg. = assemblage (*from* Galley et al. (2007); *modified from* Zwanzig (1999), and Lucas et al. (1996)).

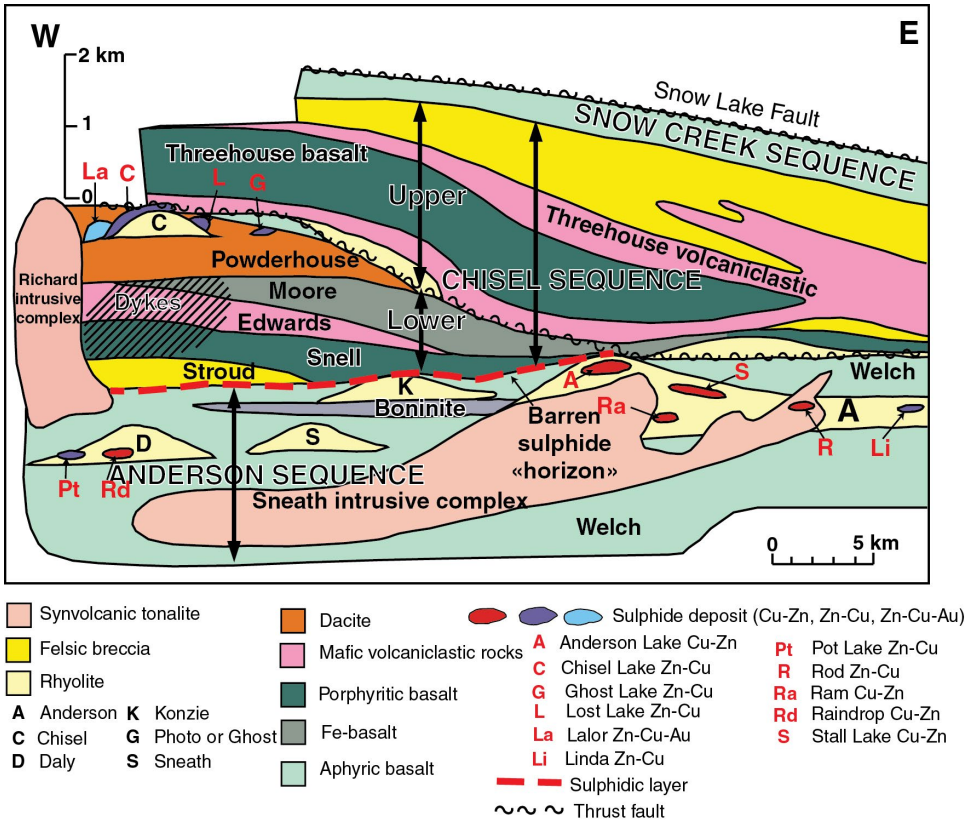

Figure 2. Schematic cross-section through the Snow Lake arc assemblage, illustrating the distribution of the main metamorphosed extrusive and synvolcanic intrusive units within the three volcanic sequences in the Snow Lake arc assemblage and their relationship to known volcanogenic massive-sulphide deposits (Bailes st al. (2013); *modified from* Bailes and Galley (1999)).

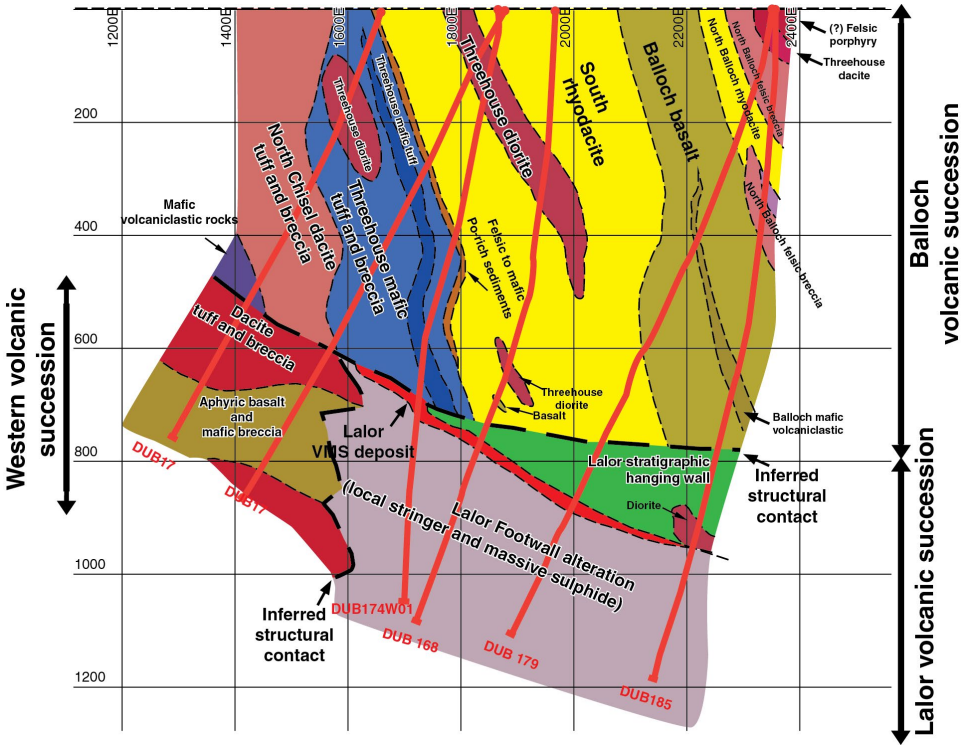

Figure 3. Geological cross-section of the Lalor deposit and surrounding rocks (looking north) showing traces of drillholes. Unit names are from A.H. Bailes (Hudbay Minerals Inc. unpub. internal report, 2008), and volcanic succession names are from this report (*modified from* A.H. Bailes, Hudbay Minerals Inc. unpub. internal report, 2009). VMS = volcanic massive-sulphide

Hudbay Minerals Inc. unpub. internal report, 2008, 2011). The contact may represent the Chisel-Lalor thrust extension in the Lalor area, but its exact nature has yet to be determined (Bailes et al., 2013; Caté et al., 2013a, b; Engelbert et al., 2014). A discrete volcanic succession herein called the "western volcanic succession" is in structural contact with the Lalor volcanic succession west of the deposit (Fig. 3). Since a large part of the hanging wall at Lalor is thought to have been transported during deformation, these rocks are not described here and the report focuses on the Lalor and western volcanic successions.

The Lalor deposit is comprised of at least 10 stacked ore lenses that are strongly flattened in the plane of the main tectonic fabric (S_{1-2}), and dip 20° to 30° toward the northeast (Fig. 4). Three types of ore lenses are present: the uppermost and southwesternmost ore zones are massive to semimassive, Zn-rich sulphide lenses; the deepest and northeasternmost lenses consist of tongue-shaped semimassive to disseminated Cu- and Au-rich sulphide bodies; and the lenses located in the intermediate levels of the ore succession are Au-rich, sulphide-poor ore zones.

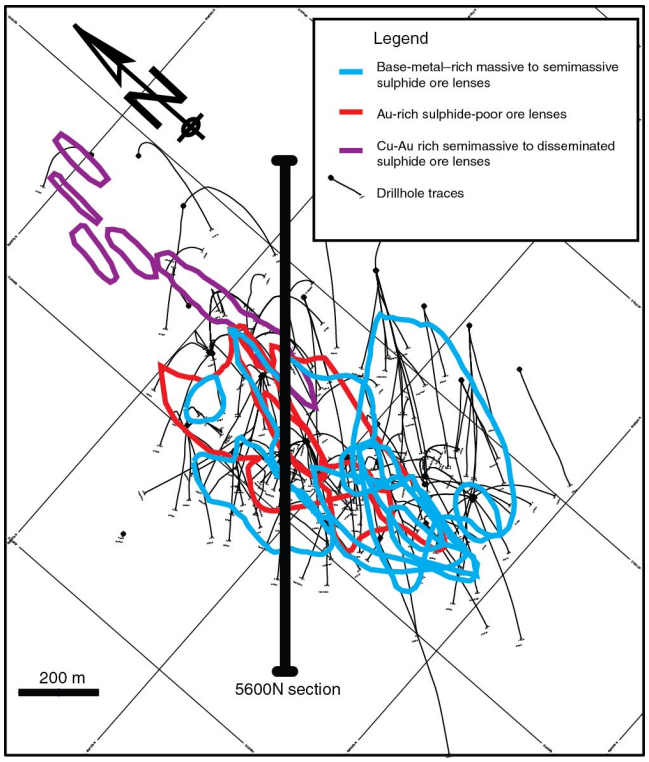

Figure 4. Plan view of the Lalor deposit showing the distribution of the base-metal, Au-rich, and Au-Cu-rich ore lenses, and traces of exploration drillholes. Each shape represents a discrete ore zone. The location of section 5600N (Fig. 5) is also shown.

Lalor host volcanic succession and metamorphosed hydrothermal alteration

The Lalor volcanic succession is composed of intensely altered volcanic rocks, and units in that package dip approximately 30° toward the east-northeast. Altered rocks are stratigraphically overlain by a weakly altered to relatively unaltered mafic unit that is structurally truncated at the contact with the Balloch volcanic succession (Fig. 5). The structural contact is gently dipping (15°) toward the northeast. Relict primary volcanic features such as amygdales, phenocrysts, or fragments are rarely present in the altered zones, and they cannot be traced across adjacent drillholes, making it very challenging to map units reliably solely with drill-core logging and underground mapping.

The hydrothermally altered rocks now consist of various metamorphic mineral assemblages that were formed during the subsequent metamorphism (syn- to late-D_2 peak amphibolite-grade metamorphism: Menard and Gordon (1997)). The metamorphic minerals are commonly very coarse due to syn- to late-D_2 metamorphic recrystallization. The presence and abundance of some key minerals such as muscovite, Mg-Fe amphibole minerals, chlorite, cordierite, Ca-amphibole minerals, and carbonate minerals define the metamorphic mineral assemblages present at Lalor. These mineral assemblages and the relative abundance and composition of key minerals can be correlated with whole-rock lithogeochemistry to define specific chemical associations. These chemical associations result from the hydrothermal alteration and subsequent metasomatism that affected the rocks during metamorphism (Menard and Gordon, 1997; Tinkham, 2013; Caté et al., 2014). Prograde metamorphism at Lalor is responsible for the dehydration of hydrothermal alteration minerals, producing metamorphic water that in turn caused partial decarbonatation (release of CO_2) through interaction with quartz and Mg-carbonate minerals (Tinkham, 2013), further texturally, chemically, and mineralogically modifying the altered volcanic and subvolcanic rocks. Thus, chemical association refers to the end product of a polyphased evolution of these rocks.

Four distinct chemical associations dominate in the Lalor alteration system: K, K-Fe-Mg, Mg-Fe, and Mg-Ca. Each of these chemical associations comprises discrete metamorphic mineral assemblages that reflect variations in the lithogeochemistry. The K chemical association is mainly present in the uppermost part of the deposit in association with the upper base-metal–rich massive-sulphide lenses (e.g. lens 10; Fig. 5). The presence of muscovite (>5%) with variable biotite, kyanite, sillimanite, and quartz are diagnostic of the K association. Pyrite is generally abundant (up to 40%) near the massive-sulphide lenses. The K-Mg-Fe chemical association is present in both the upper part of the deposit and the extensive footwall alteration zone. It is characterized by variable amounts of biotite, kyanite, sillimanite, and staurolite±garnet. Pyrite can also be abundant near the massive-sulphide lenses. The Mg-Fe chemical association is mainly present in the extensive footwall alteration zone. It is defined by the presence of Mg-Fe amphibole minerals (anthophyllite-cumingtonite series), chlorite, and/or cordierite. Garnet, staurolite, and quartz are common and

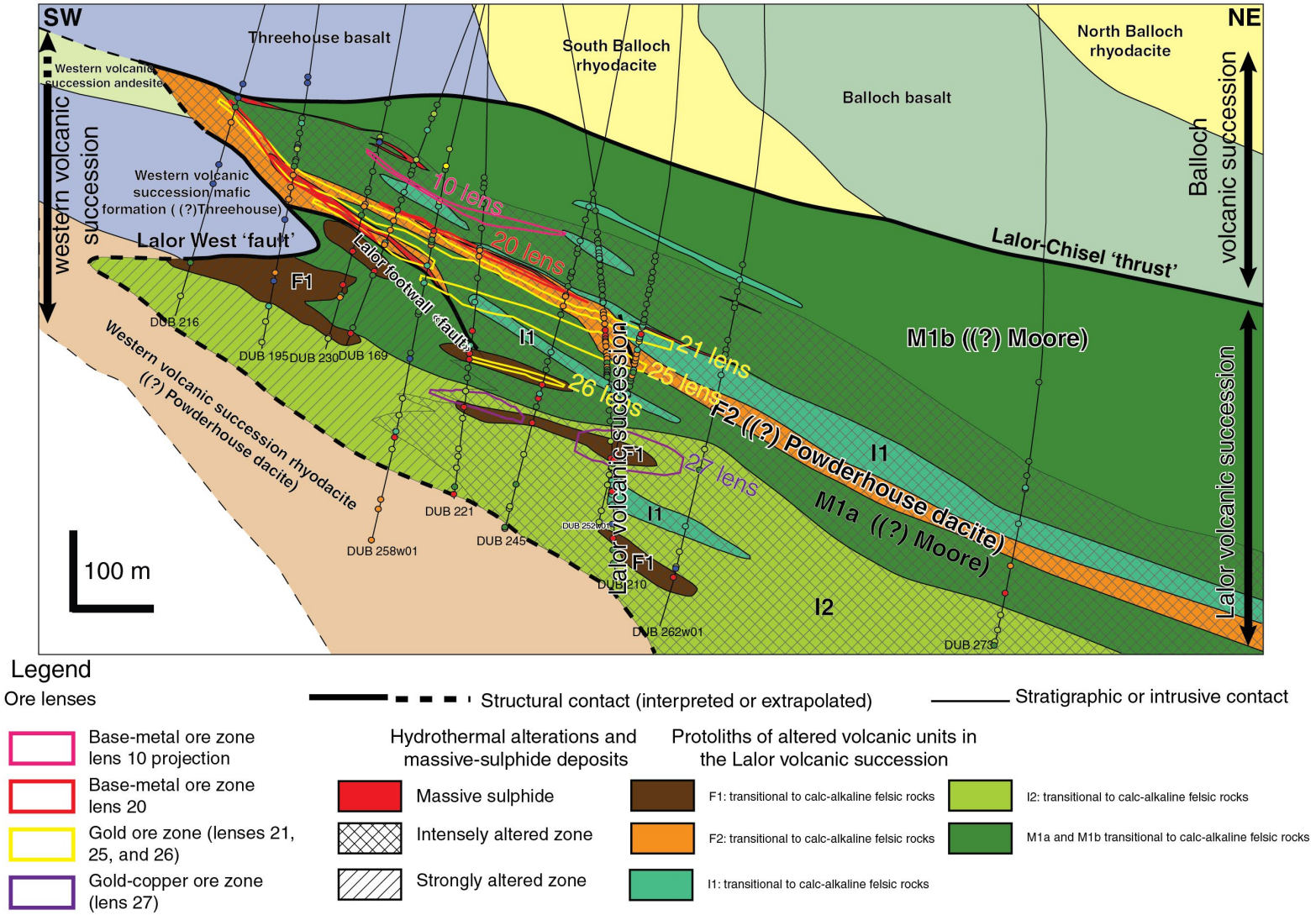

Figure 5. Simplified geological cross-section 5600N (looking northwest). The Balloch and western volcanic successions are in washed out colours and the Lalor host volcanic succession in brighter colours. Drillholes and samples (filled circles along drillholes traces) reported herein are shown, together with the distribution of the interpreted unit. Ore zone shapes determined by Hudbay Minerals Inc.; 10 lens is projected from section 5500N. Units F3, M2, and M3 are not depicted here, as they are only present in narrow intervals and in minor amounts. Unit names in the Balloch volcanic succession are from A.H. Bailes (Hudbay Minerals Inc. unpub. internal report, 2008).

can be a major (>20%) constituent of the rock, and talc is abundant locally. The Mg-Ca chemical association is associated with the lower Zn-rich massive-sulphide lenses (e.g. 20 lens; Fig. 5). It is characterized by variable amounts of Mg-chlorite, Ca-amphibole minerals (mainly actinolite series), and carbonate minerals (calcite and/or dolomite). Calcium-plagioclase, biotite, quartz, and talc are common constituents, and diopside is a major component locally.

Western volcanic succession

A succession of relatively unaltered to moderately altered volcanic rocks is present west of the Lalor deposit. These rocks dip gently (20°) toward the north-northeast (Fig. 3, 5), and are in structural contact with the Lalor volcanic succession. This contact is interpreted to be a folded early fault zone (west fault; Fig. 5). This contact, which has been mapped on all studied sections, will be the subject of a separate contribution. The lowermost observed unit in the western volcanic succession is a moderately altered rhyodacite (Fig. 5). The unit is mainly massive, with a coarse lapilli-bearing interval in its upper 40 m. Mafic dykes cut the rhyodacite, which is truncated by the west fault under the Lalor deposit. The rhyodacite is overlain by a mafic unit that consists of a series of intercalated mafic flows and volcaniclastic intervals (western volcanic succession mafic formation) (Fig. 5). The contact between the rhyodacite and the mafic rocks is demarcated by an intensely deformed, sulphide-rich horizon with well developed durchbewegung textures. The mafic volcaniclastic rocks consist of tuff to coarse monomictic lapilli-tuff units, and basalt flows contain variable amounts of plagioclase and pyroxene phenocrysts. The mafic unit is overlain by an andesitic volcaniclastic unit (western volcanic succession andesite). Since the precise location of the Lalor-Chisel contact at the top of the western volcanic succession has not been clearly established yet, it is possible that the andesitic unit is part of the Balloch volcanic succession.

LALOR HOST ROCK LEAST MOBILE ELEMENT GEOCHEMISTRY

Methods

The observations and data presented here are from a single southwest-northeast section (5600N) that crosscuts the main ore horizons (Fig. 5); however, observations and sampling along several other sections will be completed as part of the broader study and presented elsewhere. Eleven drillholes were selected over 1.2 km long distance covered by section 5600N. Drillholes have been described in detail and the NQ-size cores (diameter of 4.8 cm) were sampled from 50 m above the top of the intense alteration zone down to the end of the hole. Mineralogy, textures, structures, and contacts have systematically been documented, and volcanic facies and textures were described when preserved.

Samples were collected at variable intervals to obtain complete and representative geochemical and mineralogical data (268 samples over 4400 m of drill core) on the main lithology types (volcanic rocks, hydrothermal alteration, and metamorphic overprint). Mineralized samples are not reported on herein and will be the subject of separate contributions. A total of 268 samples of the 5600N section were analyzed for their bulk geochemical composition. Sixty-nine elements were analyzed by Activation Laboratories Inc., Ancaster, Ontario using a combination of methods that provide precise and accurate results for each element (*see* Mercier-Langevin et al. (2014, p. 269) for whole-rock lithogeochemistry analytical procedures). Precision, accuracy, and blanks were also monitored.

Results

Elements considered to be relatively immobile during volcanogenic massive-sulphide–related hydrothermal activity (i.e. Ti, Al, Ta, Nb, Hf, Zr, Y, Th, Lu, and rare-earth elements (REE) except for Eu, Winchester and Floyd (1977); Barrett and MacLean, (1994, 1999); Gifkins et al. (2005)) are used in this study to determine the distribution of, and to discriminate between the host units of the Lalor volcanic succession. All of these elements have been demonstrated to be immobile or display only minor mobility (Nb, Ta, Y, and Lu) or primary variability in volcanic rock composition. Despite their relative mobility, Si and Eu are being used in this study for comparison purposes.

Various diagrams using the aforementioned elements and element ratios are reported here to determine the nature of the volcanic rocks prior to hydrothermal alteration and metamorphism (Fig. 6, 7). As mentioned above, mapping units at Lalor is a major challenge as primary textures and features were destroyed by alteration and superimposed deformation and metamorphism. Thus, lithogeochemistry has been used to define chemostratigraphic units, which can be defined as a volcanic unit or a group of volcanic units with a similar geochemical signature and spatial distribution. The distribution of these nine chemostratigraphic units (F1, F2, F3, I1, I2, M1a, M1b, M2, and M3), the authors interpret to be volcanic or subvolcanic in origin based on distinct geochemical signatures, are shown on section 5600N (Fig. 5). To simplify the reading, these chemostratigraphic units will be referred to as units in the text.

Figure 6a shows several discrete compositional groupings that the authors interpret to be distinct units. Since SiO_2 is shown to have been mobile in most of the studied rocks (Fig. 6b), the Zr/Ti ratio is used as a proxy for determining magmatic fractionation and to discriminate units (Winchester and Floyd, 1977). The Zr/Ti ratio indicates a wide compositional range, from mafic to felsic; however, this ratio is also partly controlled by the magmatic affinity (Winchester and Floyd, 1977; Pearce, 1996), and does not always correlate with SiO_2 even in unaltered rocks (Verma et

al., 2010). Therefore, caution should be taken in inferring the magmatic differentiation of the units using Figure 6a, and more than one trace-element discrimination diagram (e.g. Fig. 6a, b) should be used to make a determination. Units F1 and F2 are felsic (rhyolitic to dacitic composition of least-altered samples on Figure 6b), but unit F2 is classified as an andesite-basalt on Figure 6a. Samples of unit F3 are all too altered to determine its primary SiO_2 compositional range, but it is most probably less fractionated than units F1 and F2 based on Zr/Ti ratio (Fig. 6a). Units I1 and I2 are, on average, andesitic based on the SiO_2 content of least altered samples (Fig. 6b). Units M1a, M1b, M2, and M3 are classified as basaltic in Figures 6a and 6b, except for a few samples of units M1a and M1b that are andesitic. Most samples on section 5600N are subalkaline in composition (Fig. 6a).

Figure 6c illustrates the magmatic affinity of volcanic rocks using a combination of immobile element ratios (Ross and Bédard, 2009); two main groups can be distinguished. Units F3, I1, M1a, and M1b have high Th/Yb values yielding a dominantly calc-alkaline affinity (magmatic trend 1). Samples of units F1, F2, and I2 have lower Th/Yb ratios and a calc-alkaline to transitional affinity (magmatic trend 2). Samples of unit M2 are tholeiitic, whereas unit M3 has a tholeiitic to transitional affinity. These two units do show clear association with the two previous groups.

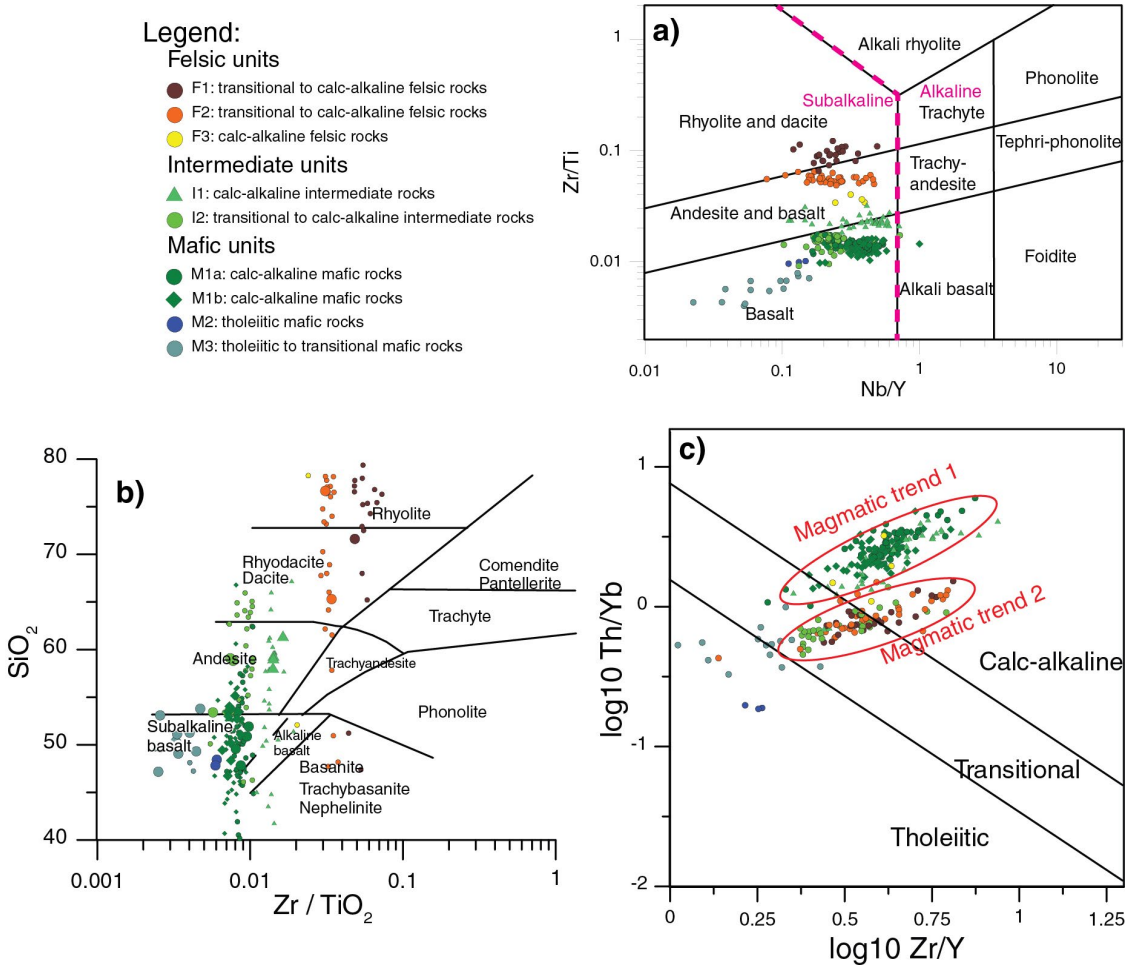

Figure 6. Trace-element discriminant diagrams of the volcanic (± intrusive) units of the Lalor succession sampled from selected drillholes along section 5600N (Fig. 5). **a)** Pearce (1996) classification diagram *modified from* Winchester and Floyd (1977). **b)** Winchester and Floyd (1977) classification diagram. Thirty-six samples with less than 40 weight per cent SiO_2 and nine samples with more than 80 weight per cent SiO_2 have been excluded as they fall out of the diagram range. As SiO_2 has been strongly affected by volcanogenic massive-sulphide alteration and vertically spreads the samples, only the SiO_2 content of the less-altered samples (wider symbols, with 20<AI<60, AI = $(MgO+K_2O)/(MgO+K_2O+Na_2O+CaO)$, S<1%, CO_2<1%, Na_2O>0.5%, LOI<2% and fresh looking texture and mineralogy) is used in this report to determine the fractionation of the units. **c)** Magmatic affinity diagram of Ross and Bédard (2009).

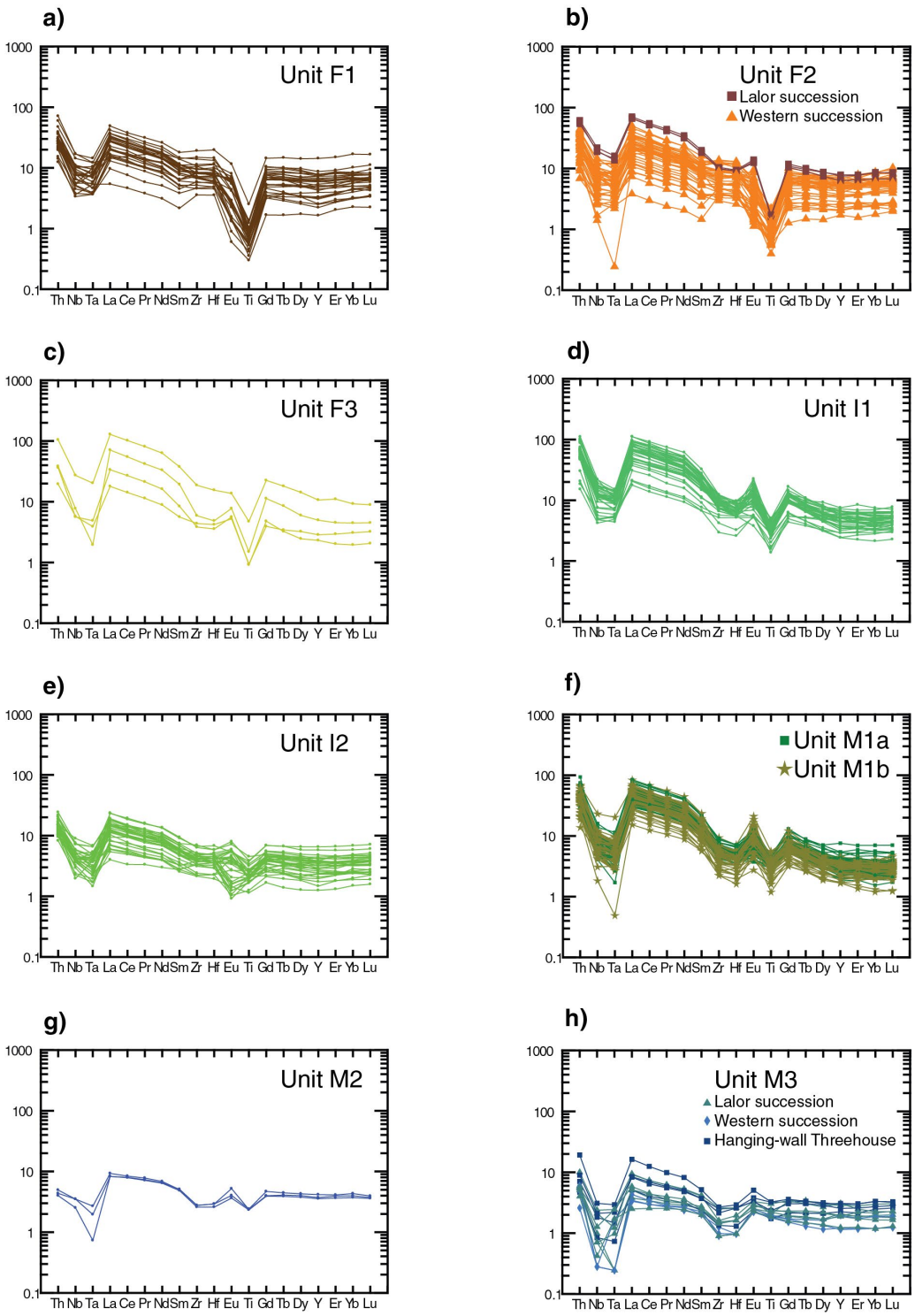

Figure 7. Primitive mantle-normalized incompatible element diagrams (Sun and McDonough, 1989) of Lalor and west volcanic successions units. **a)** Unit F1 (n = 26). **b)** Unit F2 in the Lalor volcanic succession (n = 36, two anomalous patterns are not shown with sampling-, analysis-, or alteration-related anomalies) and in the western volcanic succession (n = 3). **c)** Unit F3 (n = 4). **d)** Unit I1 (n = 37, two anomalous patterns are not shown). **e)** Unit I2 (n = 31). **f)** Units M1a (n = 43) and M1b (n = 71). **g)** Unit M2 (n = 3). **h)** Unit M3 as unaltered dykes in the Lalor volcanic succession (n = 7), flows in the western volcanic succession (n = 3), and flows in the hanging wall (Threehouse, n = 4). Large-ion lithophile elements (LILE) are not shown here due to the mobility of these elements during hydrothermal alteration (Gifkins et al., 2005).

Primitive mantle-normalized spider diagrams (Fig. 7) and several immobile high field-strength elements (HFSE) and REE ratios (Table 1; Fig. 6) vary between the different units and are used here as discriminating tools between units. Petrogenetic processes responsible for the formation of those units will be discussed in separate contributions.

Units F3, I1, M1a, and M1b have a La/Yb ratio of about 20, whereas the other units are rather characterized by average values lower than 7 (Table 1). Unit M2 has the lowest average La/Yb ratio at 3.0, followed by unit M3, at 4.1 (Table 1). The Nb/Th ratio varies between 1.4 and 1.9 on average for units F3, I1, M1a, and M1b whereas units F1, F2, and I2 have values between 2.3 and 2.7 on average (Table 1). Unit M3 has an average Nb/Th ratio of 1.5, comparable to that of units F3, I1, M1a, and M1b, whereas unit M2 has the highest average value at 6.0 (Table 1). The slope of the heavy REE portions on the primitive mantle-normalized plots (Gd, Tb, Dy, Ho, Er, and Yb) is steeper for units F3, I1, M1a, and M1b with an average Gd/Yb ratio higher than 2.6, whereas the average values are lower than 1.4 for the other units. A negative Eu anomaly only affects altered rocks and is thus considered to be due to the destruction of feldspar minerals during the volcanogenic massive-sulphide–related hydrothermal alteration (Fig. 7).

Units M1a and M1b cannot be discriminated based on geochemistry, but they are spatially distinct on section 5600N, and thus can be considered as two distinct units (Fig. 5).

Unit groupings and distribution

Two main groups of units and two distinct ungrouped units can be distinguished in the Lalor volcanic succession based on geochemical composition (Fig. 6, 7). Units F3, I1, M1a, and M1b have low Nb/Th and high Th/Yb, La/Yb, and Gd/Yb ratios (magmatic trend 1), whereas units F1, F2, and I2 have lower Th/Yb and La/Yb ratios, moderate Nb/Th, and low Gd/Yb ratios (magmatic trend 2). Units within these groups may have a common magmatic origin, but more work is necessary to decipher the magmatic evolution of the Lalor volcanic succession rocks (Fig. 5). Moreover, units from both of these groups are intercalated in the volcanic succession.

Unit M2 only occurs as dykes that crosscut both the Lalor volcanic succession and the Balloch volcanic succession. The moderate to low La/Yb and Gd/Yb ratios associated with the high Nb/Th ratios (average of 6.0) distinguish this unit from the host volcanic units of magmatic trends 1 and 2.

Unit M3 is comprised of samples of relatively unaltered mafic flows from the Balloch volcanic succession and from the western volcanic succession, as well as unaltered mafic dykes in the Lalor volcanic succession. This group of mafic rocks has well developed negative Nb-Ta anomalies and low Nb/Th values, comparable to units F3, I1, M1a, and M1b (group 1), despite moderate La/Yb and Sm/Yb ratios.

Section 5600N chemostratigraphy

The spatial distribution of the various compositional rock types provides important insight on the volcanic architecture (and subsequent structural deformation), and chemostratigraphy is therefore an essential tool to map and interpret the geology in highly hydrothermally altered, deformed, and metamorphosed sequences such as the Lalor host succession.

Western volcanic succession

The lowermost drilled unit of the western volcanic succession was sampled at three different locations on section 5600N, and has a geochemical signature similar to that of unit F2, except for slightly higher La/Yb values (11 to 13, Table 1), and on this basis is classified as part of unit F2. This rhyodacite (65–75 weight per cent SiO_2) is mainly massive with a 40 m thick interval of polymictic lapilli-bearing felsic volcaniclastic rocks at the top. The unit is weakly to moderately altered with an alteration index ($AI = 100*(MgO+K_2O)/(MgO+K_2O+CaO+Na_2O)$, Ishikawa et al. (1976)) that varies between 17 to 90, with some intervals enriched in garnet, Ca-amphibole, or muscovite, but with relatively well preserved primary textures (breccia and lapilli shapes, phenocrysts in clasts). The overlying mafic unit has been sampled in four discrete locations on section 5600N, and its composition is identical to that of unit M3. The mafic unit does not exhibit evidence of intense alteration (AI = 15 to 45). The western volcanic succession andesite has not been sampled on section 5600N.

Lalor volcanic succession

The Lalor host volcanic succession consists of a complex series of layers and lenses of volcanic units that are dipping 30° east to northeast. Most of the contacts are parallel or subparallel to the main S_{1-2} foliation (Fig. 5). Deformation is commonly more intense at or near the contact between units, hydrothermally altered rocks, and ore zones, due to rheological contrasts. Some transposition likely occurred along some of the contacts. The hanging wall of the deposit is relatively unaltered, whereas rocks in the immediate footwall are intensely altered, and zones of less intense alteration are present deeper in the footwall, which is typical of volcanogenic massive-sulphide systems, suggesting that the Lalor volcanic succession has not been overturned, although the authors' ongoing structural study will help better understand the nature and effects of the deformation on the deposit geometry.

Unit I2 is the lowermost drilled unit; it is 150 m thick on average and contains several lenses of units F1 and I1 that are perhaps intrusive, based on their distribution in small intervals that are difficult to correlate between nearby drillholes; these may be tectonically transposed and dismembered sills or dykes. The postdeformational true thickness of lenses of units F1 and I1 cannot be determined with the current

Table 1. Average chemical composition of the chemostratigraphic units of the 5600N section at the Lalor deposit. No sample of least altered F3 unit has been collected. AI = Hashimoto alteration index = 100*[(MgO+K_2O)/(MgO+K_2O+Na_2O+CaO)] (Ishikawa et al., 1976).

	F1			F2 ((?) Powderhouse dacite)				F3	
	All samples (n = 26)		Least altered (n = 1)	All samples (n = 39)		Least altered (n = 2)		All samples (n = 4)	
	Mean	Std. Dev	Mean	Mean	Std. Dev	Mean	Std. Dev	Mean	Std. Dev
SiO_2 (wt%)	68.72	16.81	71.62	61.16	21.41	70.98	5.68	46.65	21.03
TiO_2	0.18	0.09	0.23	0.26	0.10	0.27	0.02	0.44	0.34
Al_2O_3	11.08	4.46	13.32	11.45	4.43	13.01	1.41	11.53	9.02
Fe_2O_3 (total)	4.93	2.14	4.43	5.87	3.67	5.82	1.30	6.58	2.94
Fe_2O_3	1.22	1.56	0.43	1.33	1.73	1.32	0.09	1.33	0.45
FeO	3.34	1.43	3.60	4.08	2.30	4.05	1.25	4.73	2.41
MnO	0.10	0.07	0.04	0.13	0.11	0.07	0.01	0.39	0.33
MgO	7.14	6.58	2.85	8.80	7.73	2.51	1.66	10.56	5.87
CaO	3.16	4.68	2.27	4.62	5.79	4.77	0.33	13.48	12.51
Na_2O	0.30	0.54	2.73	0.22	0.29	0.83	0.31	0.15	0.08
K_2O	1.22	1.16	2.23	1.04	1.21	1.24	0.13	0.28	0.21
P_2O_5	0.02	0.02	0.03	0.05	0.02	0.06	0.00	0.11	0.04
LOI	2.80	4.32	1.11	4.72	6.23	1.31	0.60	6.90	4.70
Total	99.65	1.38	100.90	98.38	3.79	100.85	0.05	97.04	3.63
CO_2	0.74	2.98	0.09	2.39	6.08	0.55	0.38	4.55	7.59
S	0.58	0.95	0.03	1.21	1.75	0.14	0.03	1.94	1.24
Ta (ppm)	0.3	0.1	0.3	0.3	0.1	0.2	0.0	0.3	0.3
Nb	5.7	2.2	7.3	5.7	3.3	5.5	0.3	8.3	6.5
Hf	2.5	1.0	2.8	2.2	0.9	2.5	0.3	2.2	1.5
Zr	95	34	109	85	33	88	12	92	68
Ti	1061	531	1349	1557	617	1612	144	2625	2054
Y	25.6	11.2	29.4	22.6	7.0	23.8	1.7	23.7	15.1
Th	2.5	0.9	2.7	2.4	1.1	2.5	0.2	4.2	2.8
La	17.9	6.3	18.6	18.9	10.4	19.6	4.6	43.2	29.3
Ce	37.4	12.8	38.0	39.0	20.6	41.0	9.0	87.8	59.8
Pr	4.7	1.6	4.7	4.8	2.5	5.2	1.1	10.8	7.4
Nd	18.8	6.4	19.1	19.4	9.6	20.5	3.6	41.1	28.4
Sm	4.06	1.44	4.41	4.08	1.82	4.36	0.64	7.87	5.58
Eu	0.67	0.44	0.97	0.79	0.54	1.20	0.23	1.36	0.57
Gd	3.88	1.54	4.14	3.78	1.42	4.02	0.23	6.33	4.42
Tb	0.68	0.28	0.76	0.64	0.22	0.66	0.03	0.90	0.65
Dy	4.36	1.82	4.77	3.97	1.29	3.97	0.09	4.77	3.44
Ho	0.92	0.39	1.04	0.83	0.26	0.85	0.05	0.88	0.65
Er	2.87	1.21	3.33	2.50	0.76	2.65	0.10	2.46	1.69
Tm	0.458	0.191	0.531	0.396	0.124	0.432	0.018	0.348	0.221
Yb	3.16	1.33	3.68	2.72	0.87	2.94	0.08	2.31	1.37
Lu	0.489	0.199	0.564	0.428	0.142	0.454	0.011	0.346	0.192
Zr/TiO_2	0.056	0.008	0.048	0.033	0.002	0.033	0.002	0.022	0.002
Nb/Y	0.24	0.07	0.25	0.24	0.09	0.23	0.03	0.33	0.06
Th/Yb	0.84	0.22	0.73	0.86	0.24	0.84	0.10	1.94	0.80
Zr/Y	3.93	0.95	3.71	3.84	1.12	3.76	0.77	3.77	0.53
La/Yb	5.95	1.74	5.05	6.80	2.39	6.71	1.75	18.44	6.20
Gd/Yb	1.25	0.25	1.13	1.38	0.26	1.37	0.12	2.63	0.63
Nb/Th	2.27	0.39	2.71	2.34	0.60	2.21	0.11	1.91	0.45
AI	75.9	20.2	50.4	70.8	22.8	37.7	9.3	52.7	23.3
CCPI	84.1	15.7	58.0	87.6	13.4	78.0	2.9	96.7	2.1

Table 1. Continued.

	I1				I2				M1a ((?) Moore mafics)			
	All samples (n = 37)		Least altered (n = 4)		All samples (n = 31)		Least altered (n = 4)		All samples (n = 43)		Least altered (n = 5)	
	Mean	Std. Dev	Mean	Std. Dev	Mean	Std. Dev	Mean	Std. Dev	Mean	Std. Dev	Mean	Std. Dev
SiO_2 (wt%)	49.96	13.03	59.50	1.21	57.36	7.14	56.21	2.74	48.69	6.76	50.73	1.92
TiO_2	0.70	0.18	0.70	0.06	0.52	0.16	0.62	0.10	0.75	0.11	0.78	0.08
Al_2O_3	15.05	3.27	16.72	0.93	14.28	2.57	15.43	0.60	19.14	3.31	18.32	4.00
Fe_2O_3 (total)	12.71	3.85	9.16	1.13	11.90	2.31	13.82	1.15	12.86	4.27	11.68	4.26
Fe_2O_3	3.34	2.60	2.68	0.64	1.89	1.49	4.34	1.14	2.24	1.33	2.12	0.54
FeO	8.43	3.14	5.83	0.46	9.00	1.66	8.53	1.58	9.56	3.33	8.60	3.66
MnO	0.24	0.17	0.14	0.01	0.25	0.12	0.32	0.19	0.25	0.14	0.18	0.07
MgO	8.80	6.24	2.28	0.06	8.04	3.76	3.74	1.18	9.30	4.99	3.79	0.98
CaO	4.06	4.15	5.62	0.42	3.41	3.89	6.29	1.72	3.42	4.17	9.38	1.10
Na_2O	0.87	1.35	3.33	1.02	0.75	1.08	2.05	1.07	0.86	1.31	2.47	1.03
K_2O	1.28	1.25	1.59	0.27	1.06	1.10	0.96	1.20	1.47	1.24	1.17	0.55
P_2O_5	0.53	0.26	0.38	0.06	0.14	0.07	0.14	0.05	0.31	0.07	0.35	0.03
LOI	4.09	3.94	0.86	0.14	1.99	2.10	0.45	0.27	2.17	1.91	0.83	0.14
Total	98.31	4.80	100.53	0.24	99.81	0.95	100.03	0.92	99.33	1.05	99.71	1.05
CO_2	0.81	3.43	0.09	0.04	0.46	1.53	0.05	0.02	0.28	0.41	0.17	0.20
S	2.73	4.73	0.31	0.27	0.62	0.80	0.25	0.11	0.61	0.61	0.41	0.30
Ta (ppm)	0.4	0.1	0.3	0.1	0.2	0.1	0.2	0.1	0.2	0.1	0.2	0.1
Nb	8.6	3.3	4.9	2.3	3.2	1.1	4.0	1.2	5.1	1.7	5.3	1.0
Hf	2.1	0.5	2.7	0.3	1.2	0.3	1.2	0.3	1.4	0.3	1.5	0.2
Zr	97	24	102	4	45	13	45	11	65	13	69	8
Ti	4179	1089	4176	389	3119	938	3744	601	4483	681	4664	469
Y	22.1	5.9	26.8	4.0	15.1	5.2	16.2	3.5	15.6	4.9	16.3	1.5
Th	5.3	1.9	4.5	0.8	1.2	0.3	1.3	0.4	4.5	1.0	4.5	0.9
La	45.5	16.1	38.8	9.9	9.0	3.2	9.8	3.0	34.8	8.4	37.0	5.1
Ce	96.0	34.0	77.7	15.4	19.2	6.4	20.4	5.7	72.9	16.8	76.0	9.8
Pr	11.9	4.2	9.6	1.4	2.5	0.8	2.6	0.7	9.0	2.0	9.4	1.1
Nd	47.2	16.8	38.0	3.9	10.4	3.4	11.1	2.9	35.6	7.8	37.0	4.4
Sm	8.48	2.71	7.07	0.51	2.37	0.74	2.61	0.63	6.41	1.35	6.70	0.75
Eu	1.93	0.75	2.05	0.17	0.60	0.32	0.75	0.19	1.27	0.50	1.88	0.17
Gd	6.12	1.63	5.51	0.10	2.38	0.73	2.63	0.68	4.52	0.95	4.61	0.50
Tb	0.81	0.19	0.85	0.07	0.41	0.13	0.45	0.11	0.59	0.13	0.60	0.06
Dy	4.26	1.06	4.76	0.49	2.55	0.84	2.79	0.67	3.06	0.76	3.12	0.32
Ho	0.80	0.21	0.93	0.12	0.54	0.19	0.60	0.14	0.56	0.16	0.56	0.07
Er	2.30	0.64	2.74	0.37	1.62	0.54	1.75	0.38	1.62	0.48	1.62	0.18
Tm	0.338	0.096	0.407	0.055	0.253	0.085	0.274	0.060	0.239	0.075	0.238	0.031
Yb	2.28	0.61	2.74	0.35	1.72	0.56	1.84	0.39	1.59	0.52	1.57	0.16
Lu	0.350	0.090	0.411	0.054	0.265	0.088	0.280	0.056	0.244	0.073	0.240	0.023
Zr/TiO_2	0.014	0.002	0.015	0.001	0.009	0.001	0.007	0.001	0.009	0.001	0.009	0.001
Nb/Y	0.40	0.15	0.20	0.14	0.23	0.11	0.24	0.03	0.34	0.09	0.33	0.08
Th/Yb	2.46	0.98	1.73	0.58	0.73	0.18	0.72	0.05	3.02	0.97	2.83	0.37
Zr/Y	4.57	1.38	3.88	0.52	3.19	0.92	2.74	0.18	4.42	1.08	4.22	0.20
La/Yb	21.13	8.71	14.97	6.41	5.33	1.37	5.25	0.67	23.38	7.47	23.58	1.64
Gd/Yb	2.80	0.82	2.05	0.28	1.41	0.25	1.41	0.10	2.98	0.67	2.95	0.22
Nb/Th	1.66	0.51	1.04	0.28	2.72	0.72	2.90	0.25	1.17	0.38	1.25	0.33
AI	68.1	23.4	30.6	4.8	72.1	27.2	35.1	10.4	74.0	28.7	29.8	5.9
CCPI	88.1	12.3	68.1	6.0	90.3	9.1	84.3	2.7	86.4	16.5	77.5	12.8

Table 1. Continued.

	M1b ((?) Moore mafics)				M2				M3 ((?) Threehouse mafics)			
	All samples (n = 71)		Least altered (n =12)		All samples (n = 3)		Least altered (n = 2)		All samples (n = 14)		Least altered (n = 9)	
	Mean	Std. Dev	Mean	Std. Dev	Mean	Std. Dev	Mean	Std. Dev	Mean	Std. Dev	Mean	Std. Dev
SiO_2 (wt%)	47.75	10.86	51.70	2.45	47.99	0.32	48.14	0.31	48.86	4.56	50.55	1.93
TiO_2	0.70	0.16	0.76	0.08	0.51	0.01	0.52	0.01	0.49	0.11	0.50	0.11
Al_2O_3	15.50	3.16	14.47	1.12	14.95	0.36	14.75	0.27	16.60	1.97	16.46	1.18
Fe_2O_3 (total)	15.15	3.67	15.77	1.48	10.31	0.11	10.32	0.14	11.34	2.50	12.22	2.04
Fe_2O_3	4.47	3.04	3.78	0.82	2.12	0.54	1.76	0.20	3.18	1.27	2.71	1.03
FeO	9.60	3.38	10.78	0.73	7.37	0.53	7.70	0.30	7.34	2.23	8.54	1.30
MnO	0.36	0.70	0.23	0.06	0.24	0.04	0.25	0.05	0.22	0.08	0.20	0.08
MgO	7.10	4.34	5.97	1.12	10.24	0.59	9.84	0.13	5.46	1.22	5.63	1.09
CaO	5.73	4.79	7.09	1.39	12.42	0.33	12.31	0.35	12.84	5.48	11.07	1.63
Na_2O	0.70	0.82	1.40	0.62	0.75	0.37	0.90	0.37	1.61	1.25	1.98	1.22
K_2O	1.50	1.39	1.18	0.73	0.38	0.19	0.32	0.21	0.61	0.96	0.35	0.24
P_2O_5	0.29	0.09	0.32	0.06	0.10	0.00	0.10	0.00	0.13	0.06	0.13	0.04
LOI	3.65	3.83	0.75	0.39	1.33	0.46	1.01	0.11	1.65	1.65	0.99	0.49
Total	98.47	4.40	99.66	0.76	99.21	1.19	98.41	0.47	99.80	1.00	100.09	0.69
CO_2	0.91	3.46	0.15	0.18	0.04	0.01	0.05	0.02	0.84	2.16	0.22	0.19
S	3.54	4.32	0.15	0.11	0.10	0.10	0.03	0.02	0.59	0.71	0.30	0.26
Ta (ppm)	0.2	0.1	0.3	0.1	0.1	0.0	0.1	0.0	0.1	0.0	0.1	0.0
Nb	5.4	2.0	5.7	0.9	2.3	0.3	2.5	0.0	0.9	0.6	0.7	0.6
Hf	1.2	0.3	1.3	0.2	0.9	0.0	0.9	0.0	0.5	0.2	0.5	0.2
Zr	56	13	57	8	30	1	31	0	18	7	18	7
Ti	4201	942	4532	491	3077	44	3102	33	2966	654	2989	629
Y	14.1	2.8	14.9	1.8	17.3	1.1	17.9	1.0	9.8	3.0	8.9	3.0
Th	3.5	1.0	3.4	0.7	0.4	0.0	0.4	0.0	0.6	0.3	0.5	0.2
La	30.8	8.5	30.0	5.3	5.9	0.3	6.0	0.4	4.4	2.4	3.7	1.7
Ce	64.5	17.5	63.2	10.1	14.4	0.4	14.6	0.4	9.2	4.6	7.9	3.1
Pr	8.0	2.2	7.9	1.2	2.0	0.1	2.1	0.1	1.2	0.6	1.1	0.4
Nd	31.5	8.5	31.1	4.8	8.9	0.3	9.1	0.2	5.3	2.1	4.8	1.5
Sm	5.60	1.46	5.63	0.77	2.21	0.05	2.25	0.01	1.32	0.43	1.22	0.36
Eu	1.62	0.56	1.58	0.21	0.72	0.11	0.78	0.10	0.49	0.13	0.46	0.09
Gd	3.97	0.95	4.02	0.52	2.50	0.21	2.58	0.21	1.43	0.44	1.35	0.43
Tb	0.52	0.11	0.52	0.07	0.45	0.02	0.46	0.02	0.25	0.08	0.24	0.09
Dy	2.69	0.54	2.78	0.33	2.96	0.16	3.06	0.11	1.58	0.49	1.49	0.54
Ho	0.50	0.10	0.52	0.06	0.63	0.03	0.65	0.02	0.34	0.10	0.32	0.11
Er	1.45	0.29	1.51	0.16	1.87	0.09	1.93	0.04	1.00	0.30	0.93	0.32
Tm	0.214	0.044	0.225	0.028	0.293	0.023	0.309	0.012	0.157	0.052	0.144	0.057
Yb	1.44	0.29	1.53	0.19	1.97	0.12	2.05	0.09	1.06	0.35	0.98	0.38
Lu	0.220	0.049	0.231	0.031	0.278	0.011	0.284	0.008	0.162	0.051	0.150	0.057
Zr/TiO_2	0.008	0.001	0.008	0.001	0.006	0.000	0.006	0.000	0.003	0.001	0.003	0.001
Nb/Y	0.38	0.11	0.38	0.04	0.13	0.02	0.14	0.01	0.08	0.04	0.07	0.04
Th/Yb	2.45	0.60	2.25	0.44	0.19	0.00	0.19	0.00	0.54	0.16	0.53	0.10
Zr/Y	3.99	0.65	3.82	0.28	1.75	0.08	1.74	0.10	1.83	0.43	1.97	0.37
La/Yb	21.77	6.09	19.65	3.40	3.00	0.09	2.95	0.05	4.06	1.15	3.77	0.82
Gd/Yb	2.80	0.62	2.64	0.29	1.26	0.04	1.26	0.05	1.38	0.21	1.42	0.18
Nb/Th	1.56	0.41	1.69	0.19	6.00	0.60	6.35	0.40	1.45	0.73	1.27	0.63
Al	60.1	25.0	46.1	8.1	44.6	1.7	43.5	0.5	31.0	11.6	31.4	5.2
CCPI	89.6	7.3	88.5	3.4	94.6	2.2	94.1	2.6	87.8	7.5	87.6	6.9

sampling density, although their distribution is reasonably well constrained (Fig. 5). Several dykes of unaltered unit I1 have been observed in the hanging wall of the deposit and were less than 3 m thick.

Unit I2 is overlain by unit M1a, which also hosts several lenses of units F1 and I1, and this relationship indicates that these two units are probably intrusive. Unit M1a on section 5600N has an observed thickness that varies from 40 m to 130 m. The upper contact of unit M1a is concordant to the northeast and in the central part of the section; however, in the western part of the section, the moderately altered unit M1a is in sharp contact with the intensely altered unit F2. The sharp transition in the alteration styles suggests the presence of a structural (fault) contact between the two units (termed the Lalor footwall fault), and this fault also explains a re-entrant of unit F2 (and associated ore) within unit M1a to the southwest (Fig. 5).

Unit M1a is overlain by unit F2. Unit F2 is less than 50 m thick and hosts several massive-sulphide ore lenses (including 20 lens on Fig. 5). The thickening of unit F2 in the western part of the section may be caused by a tight and transposed F_{1-2} fold or by S_0-parallel faults. In the central part of the section, the felsic unit is offset by a fault. The drastic thickening of the overlying unit I1, which is not observed in unit F2, suggests a synvolcanic origin for this fault that would have formed after unit F2 deposition, but prior or during unit I1 deposition. Unit I1 is mainly present in the east side of the section and rapidly thins on the west side of the synvolcanic fault. Several samples located in the unit F2 envelope have been identified as being related to unit F1. These may be dismembered and/or discontinuous lenses of unit F1 intruding or intercalated in unit F2 (a similar relationship is observed lower in the succession within units I2 and M1a), or it may be due to primary chemical variations within unit F2.

The overlying mafic unit M1b is several hundred metres thick and is truncated by the structural top of the Lalor volcanic succession (Lalor-Chisel "thrust" on Fig. 5). The top of the volcanogenic massive-sulphide–related intense hydrothermal alteration zone is located less than 100 m above the base of unit M1b, and the transition from intensely altered to least-altered rocks is relatively abrupt (occurring over a few metres). The continuity of unit M1b above and under this transition suggests a stratigraphic contact, despite local increase in the deformation intensity. Unit M1b hosts several lenses of unit I1 that appear to be dykes in the unaltered hanging-wall rocks, but there is no unit F1 within unit M1b, which indicates that felsic volcanism ceased prior to the deposition of unit F2 in that area.

Several unaltered dykes crosscut altered and unaltered rocks of the Lalor volcanic succession. These dykes are mafic (attributed to units M1, M2, or M3) or intermediate (attributed to unit I1). This indicates the waning of calc-alkaline magmatism, and onset of dominantly tholeiitic magmatism after volcanogenic massive-sulphide deposit formation at Lalor.

Mineralization and alteration

The stratigraphic top of the zone of intensely altered rocks is within unit M1b (Fig. 5). This contact includes the 10 lens horizon, which is the uppermost base-metal ore lens. The underlying 20 lens is hosted in unit F2, indicating that it formed earlier than the 10 lens (i.e. stratigraphically stacked lenses) and that it is not a structural repetition of 10 lens. Apart from base-metal–rich 10 and 20 lenses, several gold zones are present at Lalor and some of these occur in section 5600N. The precious-metal–rich zones and horizons (lenses 21, 25, and 26) are stratigraphically located below 20 lens in intensely altered rocks. The Au-rich 25 lens is partly discordant to units M1a and F2, indicating mineralization is either transposed, synvolcanic, and discordant in nature, or is late- to postvolcanic and pre- to syndeformation. The 26 and 27 ore lenses are spatially associated with discrete (isolated) lenses of unit F1; however, 27 ore lens is considered to be part of the Cu-Au–rich ore lenses (the only one present on section 5600N) based on its metal content (Duff et al., 2013). This Cu-Au association may indicate high-temperature (>250°C) formation conditions in the core of the alteration and feeder pipes (Lydon, 1988; Ohmoto, 1996; Huston, 2000) of the Lalor volcanogenic massive-sulphide deposits.

Although most drillholes do not penetrate the base of the footwall alteration halo, there is a gradual decrease in alteration intensity in the southwest part of section 5600N, suggesting that the core of the hydrothermal alteration pipe is located, or was transposed, toward the northeast. Details on the alteration will be presented elsewhere.

DISCUSSION

Volcanic setting of the Lalor deposit in the Chisel sequence

All units in section 5600N show negative Nb, Ta, and Ti anomalies (Fig. 7), in agreement with the interpreted oceanic-arc setting for the Chisel sequence (David et al., 1996; Lucas et al., 1996; Bailes and Galley, 1999).

Besides, the Lalor deposit is thought to be at the same stratigraphic position as the Chisel and Chisel North deposits (Bailes et al., 2013 and references therein); however, there is some uncertainty with this interpretation due to the intense alteration and metamorphism of the host rocks at the Lalor deposit. The Chisel sequence type stratigraphic section comprises, from base to top, the Stroud felsic breccia (0–400 m), the Snell basalt (<500 m), the Edwards mafic breccia (<500 m), the Moore mafic volcaniclastic and basalt rocks (<1000 m), the Powderhouse dacite (<250 m), and the Ghost and Chisel rhyolite domes (<100 m) (Bailes and Galley, 1996; Fig. 2). The succession at Lalor (units I2,

M1a, F2, I1, and M1b) display many similarities in terms of spatial relationships and geochemical composition with the Chisel sequence:

- Unit I2 has an extended trace-element signature that is similar (shallow general slope and Nb, Ta, Zr, Hf, and Ti negative anomalies) to that of the Snell basalt (Fig. 8g), despite its intermediate magmatic composition (Fig. 6b).
- Unit I2 has also a similar extended trace-element signature to several samples of Edwards mafic breccia (Fig. 8f), but the former does not display the important trace-element signature variations present in the Edwards mafic volcanic rocks.
- Units M1a and M1b have identical geochemical signatures to the Moore mafic volcanic rocks (Fig. 8e).
- Units F1 and F2 are similar in pattern in many respects (moderate LREE slope, flat HREE slope, and Nb, Ta, Zr, and Hf negative anomalies) to the Powderhouse dacite and associated synvolcanic dykes, as well as the Ghost rhyolite (Fig. 8b, c, d); however, units F1 and F2 display slightly more pronounced negative Ti anomalies, and are slightly more differentiated (based on Zr/Ti ratios) than the Powderhouse dacite (Bailes and Galley, 1999, 2001). Also, the thickness of unit F2 at the Lalor deposit is significantly less than that of the Powderhouse dacite elsewhere.

Geochemical similarities between the units of the Chisel deposit sequence and those of the Lalor deposit host volcanic succession, as well as the similar stratigraphy between the Lalor area and the Chisel type section indicates that the Lalor deposit is located in the uppermost part of the lower Chisel sequence. There are, however, some marked differences between Lalor and the Chisel type section. This may be due in part to postdepositional structural deformation, but primary differences in the stratigraphic settings cannot be ruled out at this stage. The Moore basalt (i.e. units M1a and M1b) and the Powderhouse dacite-like unit (i.e. unit F2) are probably present in the host succession of the Lalor deposit; however, the Moore basalt would be present both below (M1a) and above (M1b) the Powderhouse dacite (F2). This could be explained by a major folding of the sequence (A.H. Bailes, Hudbay Minerals Inc. unpub. internal report, 2011) or by the continuation of the Moore basalt–related volcanism after the emplacement of the Powderhouse dacite–like F2 unit (although this is not recognized elsewhere in the district). The presence of unaltered unit M1b (i.e. Moore basalt) immediately above the 10 lens horizon and its associated hanging-wall alteration makes the second possibility more likely. A third possibility is that the F2 unit represents a distinct, "Moore-related" felsic unit intercalated with the basalt units; this felsic unit would be older than the Powderhouse dacite that would sit on the Moore basalt. If this interpretation is valid, the Lalor volcanogenic massive-sulphide deposit is older than the other volcanogenic massive-sulphide deposits of the Chisel sequence that sit higher in the stratigraphy. Unit I1 does not correlate with any known unit in the Chisel sequence, but it probably is a more differentiated equivalent of units M1a and M1b (i.e. Moore basalt), with very similar trace-element signatures (Fig. 7d, f). Another atypical feature of the Lalor deposit is the predominance of mafic rocks in the footwall, contrary to the other volcanogenic massive-sulphide deposits of the Chisel sequence, with unit F2 (i.e. Powderhouse dacite–like unit) being less than 50 m thick; however, the presence of unrecognized S_0-parallel faults (present elsewhere in the Snow Lake area; Bailes et al. (2013)) may have structurally modified the true thickness of the volcanic units.

At the Chisel mine, the Threehouse basalt forms the base of the upper Chisel sequence, in conformable contact with the lower Chisel sequence (Engelbert et al., 2014). At Lalor, the Threehouse unit sits above the Chisel-Lalor thrust and consists of mafic tuff and breccia (A.H. Bailes, Hudbay Minerals Inc. unpub. internal report, 2008). Moreover, the geochemical compositions of unit M3 (Fig. 7h) and the porphyritic and aphanitic textures of mafic Lalor succession–hosted dykes with this geochemical signature are similar to those of the Threehouse basalt.

Similar to the Chisel, Chisel North, Ghost, and Lost deposits (Bailes and Galley, 1999), the Lalor deposit is located in the uppermost part of the lower Chisel subsequence; however, the base-metal massive-sulphide lenses are both hosted within the probable equivalent of the Powderhouse dacite (e.g. 20 lens in unit F2) and higher in the stratigraphy, in the uppermost equivalent of the Moore basalt (e.g. 10 lens in unit M1b). There are no rhyolite domes recognized on section 5600N at Lalor, and this is in contrast with the Chisel, Chisel North, and Ghost deposits where felsic domes are present (Bailes and Galley, 1996). The 20 lens is situated within the F2 volcanic unit rather than at the contact with the overlying mafic volcanic rocks. Moore-style basaltic volcanism (unit M1b) was active after the deposition of the stratigraphically uppermost massive-sulphide lens at Lalor. Thus, unlike most of the volcanogenic massive-sulphide deposits of the Chisel sequence, the Lalor deposit is not located at the contact between the lower and upper Chisel subsequences. The upper Chisel subsequence at Lalor, with a transition to more tholeiitic rocks with flatter REE patterns (e.g. Threehouse basalt) is (was) probably located higher up in the now structurally truncated sequence. The presence of unaltered mafic dykes geochemically similar to the Threehouse basalt (i.e. unit M3) supports this hypothesis.

Setting of the western volcanic succession in the Chisel sequence

The western volcanic succession at Lalor is similar to the volcanic succession in the vicinity of the Chisel deposit described by Bailes and Galley (1996). Similarly to the F2

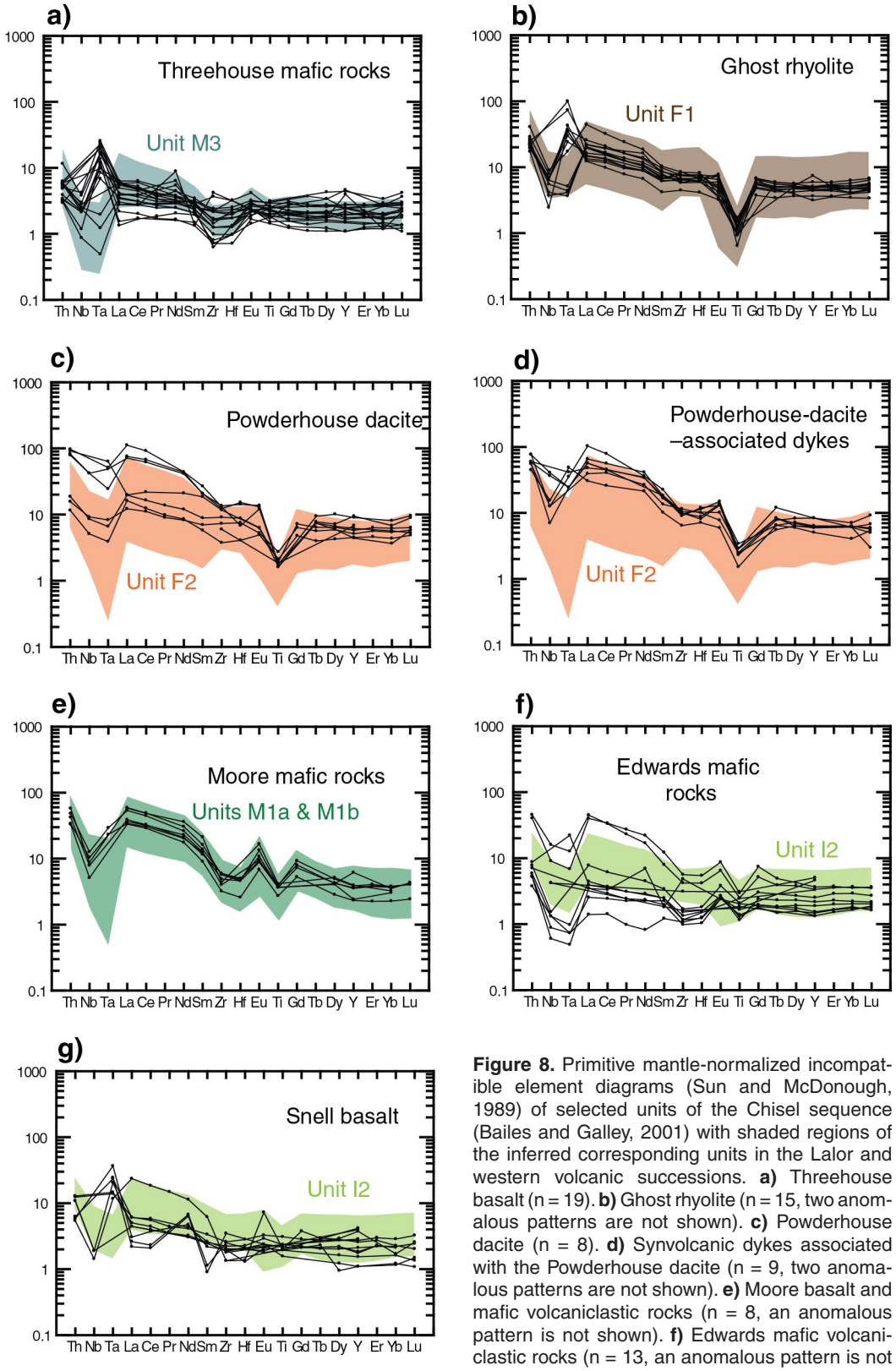

Figure 8. Primitive mantle-normalized incompatible element diagrams (Sun and McDonough, 1989) of selected units of the Chisel sequence (Bailes and Galley, 2001) with shaded regions of the inferred corresponding units in the Lalor and western volcanic successions. **a)** Threehouse basalt (n = 19). **b)** Ghost rhyolite (n = 15, two anomalous patterns are not shown). **c)** Powderhouse dacite (n = 8). **d)** Synvolcanic dykes associated with the Powderhouse dacite (n = 9, two anomalous patterns are not shown). **e)** Moore basalt and mafic volcaniclastic rocks (n = 8, an anomalous pattern is not shown). **f)** Edwards mafic volcaniclastic rocks (n = 13, an anomalous pattern is not shown). **g)** Snell basalt (n = 12). Large-ion lithophile elements (LILE) are not shown here due to the mobility of these elements during hydrothermal alteration.

unit in the Lalor volcanic succession, the rhyodacitic unit of the western succession is geochemically similar to the Powderhouse dacite, and the presence of a polymictic lapilli-bearing tuff stratigraphically overlying a massive portion of the unit is similar to the Powderhouse dacite between the Chisel and Lost deposits (Engelbert et al., 2014; Gibson et al., 2014; V. Friesen, M. Engelbert, H. Gibson, M. DeWolfe, and B. Lafrance, work in progress, 2014). Furthermore, the mafic flows and mafic volcaniclastic rocks are geochemically similar to the Threehouse mafic formation described by Bailes and Galley (1996). The stratigraphic position of this Threehouse-style mafic unit is different from its normal position in the Chisel type section; further work is currently being done to better understand this unit and its position. Thus, the Powderhouse dacite and the Threehouse-style mafic unit are both interpreted to be present in the western volcanic succession, and the contact between the two is characterized by a strongly deformed sulphide-rich horizon, with weak to moderate pervasive alteration developed in the rhyodacite, but not in the mafic rocks. Thus, the contact between the two units may be the volcanogenic massive-sulphide–bearing horizon at the contact between the lower- and upper-Chisel subsequences.

Implications for exploration

The presence of the 10 lens in unit M1b (i.e. Moore basalt) shows that the synvolcanic hydrothermal system associated in space and time with felsic volcanism in the Snow Lake area (i.e. Richard Lake pluton, Powderhouse dacite and related synvolcanic dykes, and the Chisel and Ghost rhyolite units: Bailes and Galley (1996)) continued after the deposition of unit F2 (i.e. Powderhouse dacite-like rhyodacite at the Lalor deposit). Thus, exploration should not only focus on the Powderhouse dacite horizon in the Chisel sequence, but also on mafic volcanic rocks stratigraphically overlying it.

The Lalor volcanic succession is bounded by structural contacts at its stratigraphic and structural top and toward the southwest. Thus, the continuation of the Lalor volcanic succession and volcanogenic massive-sulphide mineralization are more likely to be found toward the north, northeast, east, and southeast. The prospectivity of the less-explored western volcanic succession has yet to be determined, but the presence of a contact between Powderhouse-style felsic rocks and Threehouse-style mafic rocks suggests that this area may be highly prospective.

CONCLUSION

Use of relatively immobile element geochemical analyses (so-called chemostratigraphy), together with field observations is essential in the interpretation of the volcanic stratigraphy in the highly altered and metamorphosed Chisel sequence and other similar areas. The authors' data from the volcanic units that host the Lalor deposit show strong textural and geochemical similarities to other volcanogenic massive-sulphide deposits of the Chisel sequence (Chisel, Chisel North, Ghost, and Lost), but important differences exist (presence of the 10 lens in unit M1b (Moore-like), above unit F2 (Powderhouse-like), and absence of the Threehouse mafic rocks immediately above the deposit). These have implications for exploration, which can be extended to mafic rocks and to rocks stratigraphically under the lower Chisel–upper Chisel subsequences contact. Further studies on the stratigraphy and structural context of the Chisel basin are necessary to precisely define the stratigraphy of volcanogenic massive-sulphide–bearing horizons (e.g. M. Engelbert, V. Friesen, H. Gibson, and B. Lafrance, work in progress, 2014). Ongoing work on the Lalor deposit will allow the characterization of the primary petrotectonic setting, structural history, and hydrothermal alteration (e.g. A. Caté, P. Mercier-Langevin, S. Duff, P.-S. Ross, B. Dubé, S. Gagné, and M. Hannington, work in progress, 2014; E. Schetselaar, P. Shamsipour, K. Miah, G. Bellefleur, S. Cheraghi, J. Craven, A. Caté, P. Mercier-Langevin, N. El Goumi, R. Enkin, and M. Salisbury, work in progress, 2014), mineralizing processes (e.g. S. Duff, M. Hannington, P. Mercier-Langevin, A. Caté, work in progress, 2014), and the metamorphic evolution (e.g. J. Lam, D. Tinkham, and H. Gibson, work in progress, 2014).

ACKNOWLEDGMENTS

The authors' research at Lalor is funded by the Geological Survey of Canada (GSC) through the Targeted Geoscience Initiative 4 Program (TGI-4) and by Hudbay Minerals Inc. The activity is a GSC, Institut de la recherche scientifique–Centre Eau, Terre et Environnement, University of Ottawa, Hudbay Minerals Inc., and Manitoba Geological Survey joint project. The authors express their sincere appreciation to Hudbay Minerals Inc., especially to C. Taylor, B. Janser, J. Levers, S. Bernauer, D. Simms, and T. Schwartz for granting access to the mine, drill core, and data. This project is also done in synergy with the TGI-4 Methodology Development project (G. Bellefleur, E. Schetselaar, J. Craven, P. Shamsipour, K. Miah, and S. Cheraghi) and in collaboration with the Laurentian University research group (D. Tinkham, H. Gibson, B. Lafrance, M. Engelbert, K. Rubingh, J. Lam, and V. Friesen) in the Snow Lake area. The authors are very grateful to A. Bailes (Bailes Geoscience) and D. Tinkham for their essential help with the geology of the Snow Lake camp and metamorphic reactions and assemblages, and to K. Gilmore for his support in developing this project.

REFERENCES

Bailes, A. and Galley, A., 1996. Setting of Paleoproterozoic volcanic-hosted massive base metal sulphide deposits, Snow Lake; *in* EXTECH 1: A Multidisciplinary Approach to Massive Sulphide Research in the Rusty Lake-Snow Lake Greenstone Belts, Manitoba; Geological Survey of Canada, Bulletin 426, p. 105–138.

Bailes, A.H. and Galley, A.G., 1999. Evolution of the Paleoproterozoic Snow Lake arc assemblage and geodynamic setting for associated volcanic-hosted massive sulphide deposits, Flin Flon Belt, Manitoba, Canada; Canadian Journal of Earth Sciences, v. 36, no. 11, p. 1789–1805. doi:10.1139/e98-111

Bailes, A.H. and Galley, A.G., 2001. Geochemistry and tectonic setting of volcanic and intrusive rocks in the VMS-hosting Snow Lake area assemblage, Flin Flon Belt, Manitoba: a preliminary release of the geochemical data set; Manitoba Industry, Trade and Mines, Geological Survey, Open File Report 2001-6, 1 CD-ROM.

Bailes, A.H., Rubingh, K., Gagné, S., Taylor, C., Galley, A., Bernauer, S., and Simms, D., 2013. Volcanological and Structural Setting of Paleoproterozoic VMS and Gold Deposits at Snow Lake; Geological Association of Canada–Mineralogical Association of Canada, Winnipeg, Manitoba, May 22–25, 2013, Field Trip Guidebook FT-A2, Manitoba Geological Survey, Open File OF2013-3, 63 p.

Barrett, T.J. and MacLean, W.H., 1994. Chemostratigraphy and hydrothermal alteration in exploration for VHMS deposits in greenstones and younger volcanic rocks; *in* Alteration and Alteration Processes Associated with Ore-Forming Systems, (ed.) D.R. Lentz; Geological Association of Canada, Short Course Notes, v. 11, p. 433–466.

Barrett, T. and MacLean, W., 1999. Volcanic sequences, lithogeochemistry, and hydrothermal alteration in some bimodal volcanic-associated massive sulfide systems; *in* Volcanic Associated Massive Sulfide Deposits: Processes and Examples in Modern and Ancient Settings, (ed.) C.T. Barrie and M. Hannington; Reviews in Economic Geology, v. 8, p. 101–131.

Bernier, L., Pouliot, G., and MacLean, W.H., 1987. Geology and metamorphism of the montauban north gold zone: a metamorphosed polymetallic exhalative deposit, Grenville province, Quebec; Economic Geology and the Bulletin of the Society of Economic Geologists, v. 82, no. 8, p. 2076–2090. doi:10.2113/gsecongeo.82.8.2076

Caté, A., Mercier-Langevin, P., Ross, P.S., Duff, S., Hannington, M., Dubé, B., and Gagné, S., 2013a. Preliminary observations on the geological environment of the Paleoproterozoic auriferous volcanogenic massive sulphide deposit of Lalor, Snow Lake, Manitoba; Geological Survey of Canada, Open File 7372, 13 p. doi:10.4095/292516

Caté, A., Mercier-Langevin, P., Ross, P.S., Duff, S., Hannington, M., Dubé, B., and Gagné, S., 2013b. The Paleoproterozoic Lalor VMS deposit, Snow Lake, Manitoba: preliminary observations on the nature and architecture of the gold- and base metal-rich ore and alteration zones; Geological Survey of Canada, Open File 7483, 19 p. doi:10.4095/293116

Caté, A., Mercier-Langevin, P., Ross, P.S., Duff, S., Hannington, M., Dubé, B., and Gagné, S., 2014. Deciphering the multiple hydrothermal, metasomatic and structural events responsible for the formation and post-depositional evolution of the Paleoproterozoic Lalor auriferous VMS deposit, Snow Lake, Manitoba; *in* Proceedings Geological Association of Canada–Mineralogical Association of Canada annual meeting, May 20–22, 2014, Fredericton, New Brunswick, p. 83–84.

Corrigan, D., Pehrsson, S., Wodicka, N., and de Kemp, E., 2009. The Palaeoproterozoic Trans-Hudson Orogen: a prototype of modern accretionary processes; *in* A. Orogens and M. Analogues, (ed.) J.B. Murphy, J.D. Keppie, and A.J. Hynes; Geological Society, London, Special Publications, v. 327, p. 457–479. doi:10.1144/SP327.19

David, J., Bailes, A.H., and Machado, N., 1996. Evolution of the Snow Lake portion of the Palaeoproterozoic Flin Flon and Kisseynew belts, Trans-Hudson Orogen, Manitoba, Canada; Precambrian Research, v. 80, no. 1–2, p. 107–124. doi:10.1016/S0301-9268(96)00008-3

Duff, S., Caté, A., Hannington, M., Mercier-Langevin, P., and Ross, P.-S., 2013. Major ore types of the Lalor Deposit, Snow Lake, Manitoba; Geological Society of America Abstracts with Programs, v. 45, no. 7, p. 806.

Engelbert, M.S., Friesen, V., Gibson, H., and Lafrance, B., 2014. Volcanic reconstruction of the productive VMS ore interval in the Paleoproterozoic Chisel sequence, Snow Lake, Manitoba; *in* Proceedings Geological Association of Canada–Mineralogical Association of Canada annual meeting, May 20–22, 2014, Fredericton, New Brunswick, p. 83–84.

Froese, E. and Gasparrini, E., 1975. Metamorphic zones in the Snow Lake area, Manitoba; Canadian Mineralogist, v. 13, no. 2, p. 162–167.

Galley, A.G., Bailes, A.H., and Kitzler, G., 1993. Geological setting and hydrothermal evolution of the Chisel Lake and North Chisel Zn-Pb-Cu-Ag-Au massive sulfide deposits, Snow Lake, Manitoba; Exploration and Mining Geology, v. 2, no. 4, p. 271–295.

Galley, A.G., Syme, R., and Bailes, A.H., 2007. Metallogeny of the Paleoproterozoic Flin Flon Belt, Manitoba and Saskatchewan, *in* Mineral Deposits of Canada: A Synthesis of Major Deposit Types, District Metallogeny, The Evolution of Geological Provinces, and Exploration Methods (ed.) W.D. Goodfellow; Geological Association of Canada, Mineral Deposits Division, Special Publication, v. 5, p. 509–531.

Gibson, H.L., Morton, R.L., and Hudak, G.J., 1999. Submarine volcanic processes, deposits, and environments favorable for the location of volcanic-associated massive sulfide deposits; *in* Volcanic Associated Massive Sulfide Deposits: Processes and Examples in Modern and Ancient Settings, (ed.) C.T. Barrie and M.D. Hannington; Reviews in Economic Geology, v. 8, p. 13–48.

Gibson, H., Engelbert, M.S., Lafrance, B., Friesen, V., DeWolfe, M., Tinkham, D.K., and Bailes, A.H., 2014. Reconstruction of the ore interval and environment for the Paleoproterozoic, Lost and Ghost Lake VMS deposits, Snow Lake, Manitoba; *in* Proceedings Geological Association of Canada–Mineralogical Association of Canada annual meeting, May 20–22, 2014, Fredericton, New Brunswick, p. 102.

Gifkins, C., Herrmann, W., and Large, R.R., 2005. Altered volcanic rocks: a guide to description and interpretation; Centre for Ore Deposit Research; University of Tasmania, Hobart, Tasmania, Australia, 275 p.

Hudbay Minerals Inc, 2014. <http://www.hudbayminerals.com/English/Home/default.aspx> [accessed April 1, 2014].

Huston, D.L., 2000. Gold in volcanic-hosted massive sulfide deposits; distribution, genesis, and exploration; *in* Gold in 2000, (ed.) S.G. Hagemann and P.E. Brown; Reviews in Economic Geology, v. 13, p. 401–426.

Ishikawa, Y., Sawaguchi, T., Iwaya, S., and Horiuchi, M., 1976. Delineation of prospecting targets for Kuroko deposits based on modes of volcanism of underlying dacite and alteration haloes; Mining Geology, v. 26, p. 105–117.

Koo, J. and Mossman, D.J., 1975. Origin and metamorphism of the Flin Flon stratabound Cu-Zn sulfide deposit, Saskatchewan and Manitoba; Economic Geology and the Bulletin of the Society of Economic Geologists, v. 70, no. 1, p. 48–62. doi:10.2113/gsecongeo.70.1.48

Kraus, J. and Williams, P.F., 1999. Structural development of the Snow Lake Allochthon and its role in the evolution of the southeastern Trans-Hudson Orogen in Manitoba, central Canada; Canadian Journal of Earth Sciences, v. 36, no. 11, p. 1881–1899. doi:10.1139/e99-014

Lam, J., Tinkham, D.K., and Gibson, H., 2013. Identification of metamorphic assemblages and textures associated with gold mineralization at the Lalor deposit, Snow Lake, MB; *in* Proceedings Geological Association of Canada–Mineralogical Association of Canada annual meeting, May 22–24, 2013, Winnipeg, Manitoba, p. 127.

Lam, J., Tinkham, D.K., and Gibson, H., 2014. Characterization of gold occurrences with respect to metamorphism at the Lalor deposit, Snow Lake, MB; *in* Proceedings Geological Association of Canada–Mineralogical Association of Canada annual meeting, May 20–22, 2014, Fredericton, New Brunswick, p. 150–151.

Lucas, S.B., Stern, R.A., Syme, E.C., Reilly, B.A., and Thomas, D.J., 1996. Intraoceanic tectonics and the development of continental crust: 1.92–1.84 Ga evolution of the Flin Flon Belt, Canada; Geological Society of America Bulletin, v. 108, no. 5, p. 602–629. doi:10.1130/0016-7606(1996)108<0602:ITATDO>2.3.CO;2

Lydon, J.W., 1988. Ore deposit models 14. Volcanogenic massive sulphide deposits. Part 2: genetic models; Geoscience Canada, v. 15, no. 1, p. 43–65.

MacLean, W.H. and Barrett, T.J., 1993. Lithogeochemical techniques using immobile elements; Journal of Geochemical Exploration, v. 48, no. 2, p. 109–133. doi:10.1016/0375-6742(93)90002-4

Menard, T. and Gordon, T.M., 1997. Metamorphic P-T paths from the eastern Flin Flon belt and Kisseynew domain, Snow Lake, Manitoba; Canadian Mineralogist, v. 35, no. 5, p. 1093–1115.

Mercier-Langevin, P., Dubé, B., Hannington, M.D., Davis, D.W., Lafrance, B., and Gosselin, G., 2007a. The LaRonde Penna Au-rich volcanogenic massive sulfide deposit, Abitibi Greenstone Belt, Quebec: Part I. Geology and geochronology; Economic Geology and the Bulletin of the Society of Economic Geologists, v. 102, no. 4, p. 585–609. doi:10.2113/gsecongeo.102.4.585

Mercier-Langevin, P., Dubé, B., Hannington, M.D., Richer-Laflèche, M., and Gosselin, G., 2007b. The LaRonde Penna Au-rich volcanogenic massive sulfide deposit, Abitibi Greenstone Belt, Quebec: Part II. Lithogeochemistry and paleotectonic setting; Economic Geology and the Bulletin of the Society of Economic Geologists, v. 102, no. 4, p. 611–631. doi:10.2113/gsecongeo.102.4.611

Mercier-Langevin, P., Lafrance, B., Bécu, V., Dubé, B., Kjarsgaard, I., and Guha, J., 2014. The Lemoine auriferous volcanogenic massive sulfide deposit, Chibougamau camp, Abitibi Greenstone Belt, Quebec, Canada: geology and genesis; Economic Geology and the Bulletin of the Society of Economic Geologists, v. 109, no. 1, p. 231–269. doi:10.2113/econgeo.109.1.231

Ohmoto, H., 1996. Formation of volcanogenic massive sulfide deposits: the Kuroko perspective; Ore Geology Reviews, v. 10, no. 3–6, Special Issue, p. 135–177.

Pearce, J.A., 1996. A user's guide to basalt discrimination diagrams; *in* Trace Element Geochemistry of Volcanic Rocks: Applications for Massive Sulphide Exploration, (ed.) D.A. Wyman; Geological Association of Canada, Short Course Notes, p. 79–113.

Ross, P.S. and Bédard, J.H., 2009. Magmatic affinity of modern and ancient subalkaline volcanic rocks determined from trace-element discriminant diagrams; Canadian Journal of Earth Sciences, v. 46, no. 11, p. 823–839. doi:10.1139/E09-054

Sun, S.-S. and McDonough, W.F., 1989. Chemical and isotopic systematics of oceanic basalts: implications for mantle composition and processes; Geological Society of London, Special Publications, v. 42, p. 313–345. doi:10.1144/GSL.SP.1989.042.01.19

Tinkham, D.K., 2013. A model for metamorphic devolatilization in the Lalor deposit alteration system, Snow Lake, MB; *in* Proceedings Geological Association of Canada–Mineralogical Association of Canada annual meeting, May 22–24, 2013,Winnipeg, Manitoba, p. 187.

Verma, S.P., Rodriguez-Rios, R., and Gonzalez-Ramirez, R., 2010. Statistical evaluation of classification diagrams for altered igneous rocks; Turkish Journal of Earth Sciences, v. 19, no. 2, p. 239–265.

Winchester, J.A. and Floyd, P.A., 1977. Geochemical discrimination of different magma series and their differentiation products using immobile elements; Chemical Geology, v. 20, no. C, p. 325–343. doi:10.1016/0009-2541(77)90057-2

Zheng, Y.C., Gu, L., Tang, X., Wu, C., Li, C., and Liu, S., 2011. Geology and geochemistry of highly metamorphosed footwall alteration zones in the Hongtoushan volcanogenic massive sulfide deposit, Liaoning Province, China; Resource Geology, v. 61, no. 2, p. 113–139. doi:10.1111/j.1751-3928.2011.00154.x

Zwanzig, H.V., 1999. Structure and stratigraphy of the south flank of the Kisseynew Domain in the Trans-Hudson Orogen, Manitoba: implications for 1.845–1.77 Ga collision tectonics; Canadian Journal of Earth Sciences, v. 36, no. 11, p. 1859–1880. doi:10.1139/e99-042

Geological Survey of Canada Project 340321NU61